

Review

Interface regulation and electrolyte design strategies for zinc anodes in high-performance zinc metal batteries

Xun Guo,¹ Shaoce Zhang,¹ Hu Hong,¹ Shixun Wang,¹ Jiaxiong Zhu,¹ and Chunyi Zhi^{1,2,*}¹Department of Materials Science and Engineering, City University of Hong Kong, 83 Tat Chee Avenue, Kowloon, Hong Kong 999077, P.R. China²Center for Advanced Nuclear Safety and Sustainable Development, City University of Hong Kong, Kowloon, Hong Kong 999077, P.R. China

*Correspondence: cy.zhi@cityu.edu.hk

<https://doi.org/10.1016/j.isci.2025.111751>

SUMMARY

Rechargeable zinc metal batteries (ZMBs) represent a promising solution for large-scale energy storage due to their safety, cost-effectiveness, and high theoretical capacity. However, the development of zinc metal anodes is hindered by challenges such as dendrite formation, hydrogen evolution reaction (HER), and low Coulombic efficiency stemming from undesirable interfacial processes in aqueous electrolytes. This review explores various strategies to enhance zinc anode performance, focusing on artificial SEI, morphology adjustments, electrolyte regulation, and flowing electrolyte. These approaches aim to suppress dendrite growth, mitigate side reactions, and optimize the electric double layer (EDL) and Zn^{2+} solvation structures. By addressing these interfacial challenges, the insights presented here pave the way for designing high-performance ZMBs, offering directions for future research into scalable and sustainable battery technologies.

INTRODUCTION

Electrical energy can be generated through various methods, including thermal, hydroelectric, wind, solar, and nuclear power, all of which involve converting other forms of energy into electricity. However, due to the inability of conventional materials to store electrical energy for extended periods without consumption, collecting and storing surplus energy becomes crucial. Among energy storage technologies such as pumped hydro, flywheels, compressed air, and secondary batteries, the latter stands out for its flexibility and wide applicability across diverse scenarios.

The US Department of Energy's "Energy Storage Grand Challenge" highlights secondary battery technologies such as lithium-ion, sodium-based, lead-acid, and zinc-based batteries and others as pivotal for bidirectional power storage systems. Although lithium-ion batteries dominate due to their high energy density, safety concerns have shifted attention toward aqueous batteries, which use water as the electrolyte medium. Aqueous options include lead-acid, all-vanadium flow batteries, aqueous lithium-ion and sodium-ion batteries, and nickel-metal hydride batteries.^{1,2} However, challenges such as environmental pollution from lead-acid batteries, the high cost of vanadium flow systems, low energy densities of aqueous lithium-ion and sodium-ion batteries, and the expense of nickel-metal hydride batteries leave no aqueous battery fully meeting energy storage standards.³

Aqueous zinc metal batteries (ZMBs) belong to the category of aqueous metal-ion batteries. The radius of Zn^{2+} is similar to that

of Li^+ , suggesting that Zn^{2+} can intercalate into suitable materials for storage.⁴ The standard electrode potential of Zn^{2+} relative to the standard hydrogen electrode is -0.76V , which, when paired with appropriate cathodes, yields a favorable electromotive force for the full batteries. Compared to metal electrodes with more negative electrode potentials, such as magnesium and aluminum, zinc metal exhibits relatively mild hydrogen evolution side reactions during deposition in aqueous electrolytes due to its higher hydrogen evolution overpotential. This characteristic makes zinc metal a more suitable anode for aqueous metal-ion batteries. In addition to the advantages of suitable ionic radius and electrode potential, zinc metal possesses other excellent characteristics, such as low cost and an exceptionally high theoretical volumetric capacity (5585 mAh/cm^3).^{5,6} However, developing secondary energy batteries demands enhanced system reversibility and stability.⁷

The structure of current aqueous ZMBs is shown in Figure 1A.^{8,9} The cathode in ZMBs, similar to those in lithium-ion batteries, is composed of materials capable of the reversible intercalation and deintercalation of Zn^{2+} ions, including manganese oxide (MnO_2), vanadium oxides, Prussian blue analogs, and organic cathodes. The aqueous electrolyte is typically prepared by co-dissolving zinc salts [such as ZnSO_4 , ZnCl_2 , and $\text{Zn}(\text{CF}_3\text{SO}_3)_2$] with water and organic solvents, resulting in a generally neutral or mildly acidic solution. On the anode side, zinc metal undergoes dissolution-deposition reactions throughout cycling. Although the energy density of aqueous ZMBs is relatively lower than that of state-of-art lithium-ion batteries, it remains higher than that of lead-acid batteries. Given



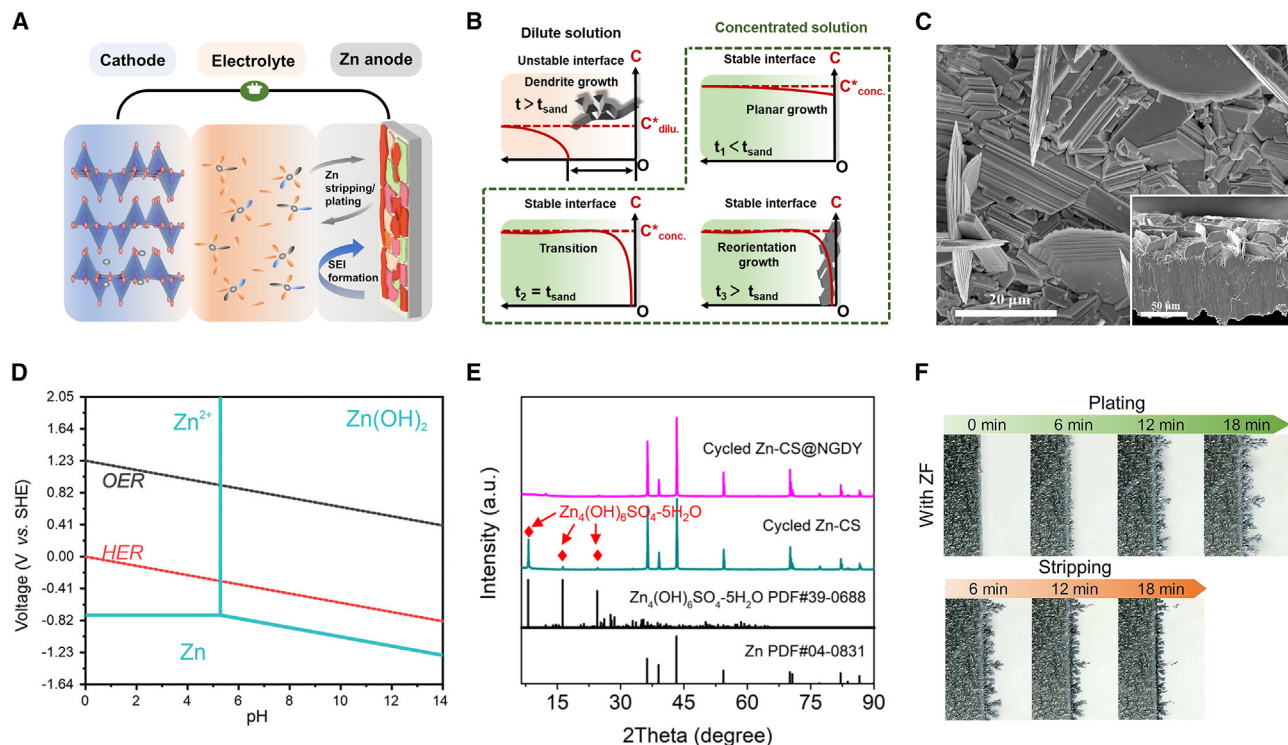


Figure 1. Challenges faced by zinc metal

(A) Schematic of complete transfer of Zn²⁺ charge carriers in full cells.⁹
 (B) Differences between electrodeposition morphology and ion concentration in dilute and concentrated electrolytes.¹⁰
 (C) SEM imaging of Zn metal after cycling in a Zn||Zn symmetric cell. The inset shows the cross-sectional views of Zn foils.⁹ Copyright 2024 Elsevier Ltd.
 (D) Pourbaix diagram of Zn in a 2 mol L⁻¹ ZnSO₄ solution.¹¹ Copyright 2021 Wiley-VCH GmbH.
 (E) XRD patterns of cycled Zn anode interfaces.¹² Copyright 2021 Wiley-VCH GmbH.
 (F) *In situ* optical images of Zn plating/stripping process.¹³ Copyright 2024 Wiley-VCH GmbH.

their extremely low cost, non-toxic nature, and safety, aqueous ZMBs hold significant potential for future development in large-scale energy storage applications. This potential is one of the reasons why this emerging field, despite its only decade-long history, has attracted significant interest from researchers.

Despite these advantages, practical deployment of ZMBs is hindered by key interfacial challenges, including dendrite growth, hydrogen evolution reactions (HER), and parasitic side reactions at the zinc metal anode. In this review, we focus on interface regulation and electrolyte design strategies as two critical pathways to address the interfacial challenges in aqueous ZMBs. By systematically analyzing the successes, limitations, and underlying mechanisms of these strategies, we aim to provide a comprehensive understanding of current advancements and identify future research directions.

ISSUES WITH ZINC ANODES

Zinc dendrites

The basic principle of dendrite growth stems from the deposition theory of metal ions at the solid-liquid interface. Traditional mass transfer theory posits that dendrite growth results from morphological and kinetic instabilities, leading to uneven mass transfer—generally, cations deposit on the solid surface

through diffusion, charge transfer, and nucleation growth stages. The rate of charge transfer depends on the intensity of the applied current. Typically, the charge transfer rate is much higher than the diffusion rate, forming a concentration gradient of cations from the bulk phase to the interface region. When the applied current density exceeds the diffusion limiting current density, over time, an "ion depletion space charge layer" forms on the surface as bulk cations fail to replenish the depleted surface layer in time (Figure 1B).^{10,14} This time is referred to as "Sand's time." The strong electro-negative electric field at the interface attracts a large number of metal ions, eventually forming the classic dendritic structure.¹⁵ This theory aligns well with experimental observations under high current densities. However, experiments have shown that metal deposition can exhibit dendritic morphology even at low current densities. One theory suggests that the intrinsic inhomogeneity of the metal surface leads to this result. Protruding parts of the metal surface with higher curvature enhance the local electric field, attracting more metal ions and thus exacerbating inhomogeneity, ultimately evolving into dendritic morphology.¹⁶ Dendrites can locally puncture the separator, leading to direct contact between the cathode and anode, causing intense heat generation, significantly compromising battery stability, and ultimately resulting in battery failure.

Similar to the challenges faced by lithium metal anodes in practical applications, zinc metal anodes also encounter significant issues with dendrites. Figure 1C shows the morphology of zinc dendrites.¹⁷ Related to the hexagonal close-packed (hcp) crystal structure of zinc metal,¹⁸ zinc dendrites typically form a two-dimensional hexagonal plate-like structure, setting their dendritic formation characteristics apart from those of traditional alkali metal anodes (Li, Na, K). Dendrite growth is influenced by various factors, including temperature, electrolyte concentration, and the inherent heterogeneity and ion transfer kinetics of the solid electrolyte interface (SEI).^{9,10,19,20} These factors primarily affect dendrite growth by influencing ion diffusion and mass transfer processes. However, existing theories struggle to integrate these factors into a unified theory. With continued theoretical exploration and advances in characterization techniques, we may gain a deeper understanding of dendrite growth in the future.

It is important to emphasize that even if a short circuit occurs within aqueous electrolytes, the electrolyte will neither ignite nor explode, ensuring the overall safety of the battery. This provides greater tolerance for potential zinc dendrite formation during cycling, making zinc metal anodes more feasible for practical battery applications than lithium metal anodes.

Low reversibility

The reversibility of zinc metal anodes is often unsatisfactory due to factors such as HER, interfacial passivation, and the formation of “dead zinc.” In neutral to mildly acidic aqueous zinc-ion electrolytes, zinc anodes typically exhibit Coulombic efficiencies below 90%, falling significantly short of the standards required for commercial applications. One reason for the low Coulombic efficiency is the inherent characteristics of aqueous electrolytes. As shown in Figure 1D, the potential-pH diagram for Zn^{2+}/Zn based on the Nernst equation indicates that under thermodynamic conditions, the electrode potential of Zn/Zn^{2+} is lower than the standard hydrogen potential across the entire pH range.¹¹ Even considering the hydrogen evolution overpotential, the HER inevitably occurs before the zinc deposition reaction in typical aqueous electrolytes. The hydrogen produced by HER dissipates from the battery system and cannot reversibly return to the solution, thereby reducing the efficiency of the battery system. Simultaneously, HER leaves OH^- ions in the solution, raising the local pH at the electrode surface. In specific zinc salt solutions, an increase in pH leads to the formation of ZnO or low-solubility, low-conductivity basic zinc salt $\text{Zn}(\text{OH})_2\text{A}_2\text{nH}_2\text{O}$,²¹ where A represents anions such as SO_4^{2-} or CF_3SO_3^- (Figure 1E). These passivating byproducts cover the zinc anode surface, blocking contact between the zinc anode and the electrolyte, significantly increasing the battery's impedance and hindering the efficient deposition of zinc ions. As the cycle number increases, the electrolyte is gradually depleted, and passivating inert byproducts accumulate, ultimately leading to battery failure.

Another factor contributing to low reversibility is the formation of “dead zinc,” which originates from the inherent properties of zinc dendrites.¹⁸ As illustrated in Figure 1F, the sections of zinc dendrites near the anode surface experience significant stress, rendering them fragile and susceptible to breaking under

external disturbances. These detached zinc particles lose electrical connectivity and fall off, becoming “dead zinc” that cannot participate in subsequent electrochemical reactions, thereby reducing the overall efficiency of the battery system.

It is important to note that dendrites and low reversibility are not independent issues but are closely interrelated. The sharp tips of zinc dendrites induce localized electric field enhancements, which accelerate HER and interfacial side reactions, consuming active materials and electrolytes, and thereby reducing Coulombic efficiency and overall reversibility. Conversely, poor interfacial stability and side reactions, which manifest as low cycling reversibility, result in uneven zinc ion flux and irregular zinc deposition, further promoting dendrite growth. Zinc dendrites and low reversibility form a feedback loop, where one issue aggravates the other.

OPTIMIZATION STRATEGIES FOR ZINC ANODES

The issues of zinc dendrites and low reversibility are the primary factors limiting the practical application of zinc anodes. From the aforementioned exploration, it can be observed that controlling zinc dendrites requires managing the diffusion and transport of zinc ions at the interface or the nucleation and growth process. Enhancing the reversibility of zinc metal requires effectively reducing the interfacial HER kinetics and preventing the formation of “dead zinc.” Overall, optimization strategies can be categorized into four main approaches: artificial SEI on zinc anodes, morphological and structural adjustments of zinc anodes, electrolyte regulation, and flowing electrolyte.

Artificial SEI on zinc anodes

The SEI is a solid byproduct generated from electron exchange between the metal and electrolyte, exhibiting characteristics similar to liquid electrolytes in that it conducts ions but insulates electrons. With its independent phase structure, the SEI isolates the metal from the electrolyte, preventing further side reactions and allowing standard electrode reactions to proceed. However, in aqueous ZMBs, basic salt byproducts on the zinc anode surface accumulate loosely, failing to isolate the zinc metal from the electrolyte effectively and thus unable to prevent side reactions. Consequently, researchers have turned to artificial SEI layers to isolate the electrolyte from the metal anode, thereby reducing unwanted side reactions and improving the reversibility of zinc metal. Applying an artificial SEI on the zinc anode surface can also inhibit dendrite formation by creating a barrier that regulates zinc ion flow. Research on artificial SEI layers for zinc metal can be broadly categorized into organic, inorganic, and metallic materials.

Organic materials, including polymeric materials,^{22–24} metal-organic frameworks (MOFs),^{25,26} and covalent organic frameworks (COFs),^{27–30} offer several advantages for zinc metal anodes. Specific functional groups can be precisely designed through chemical synthesis to form a stable SEI with zinc metal. These functional groups optimize Zn^{2+} transport, enhance charge transfer kinetics, reduce nucleation overpotential, and inhibit dendrite growth, effectively suppressing side reactions and corrosion.³¹ Additionally, organic materials exhibit excellent interfacial adaptability, maintaining strong adhesion and

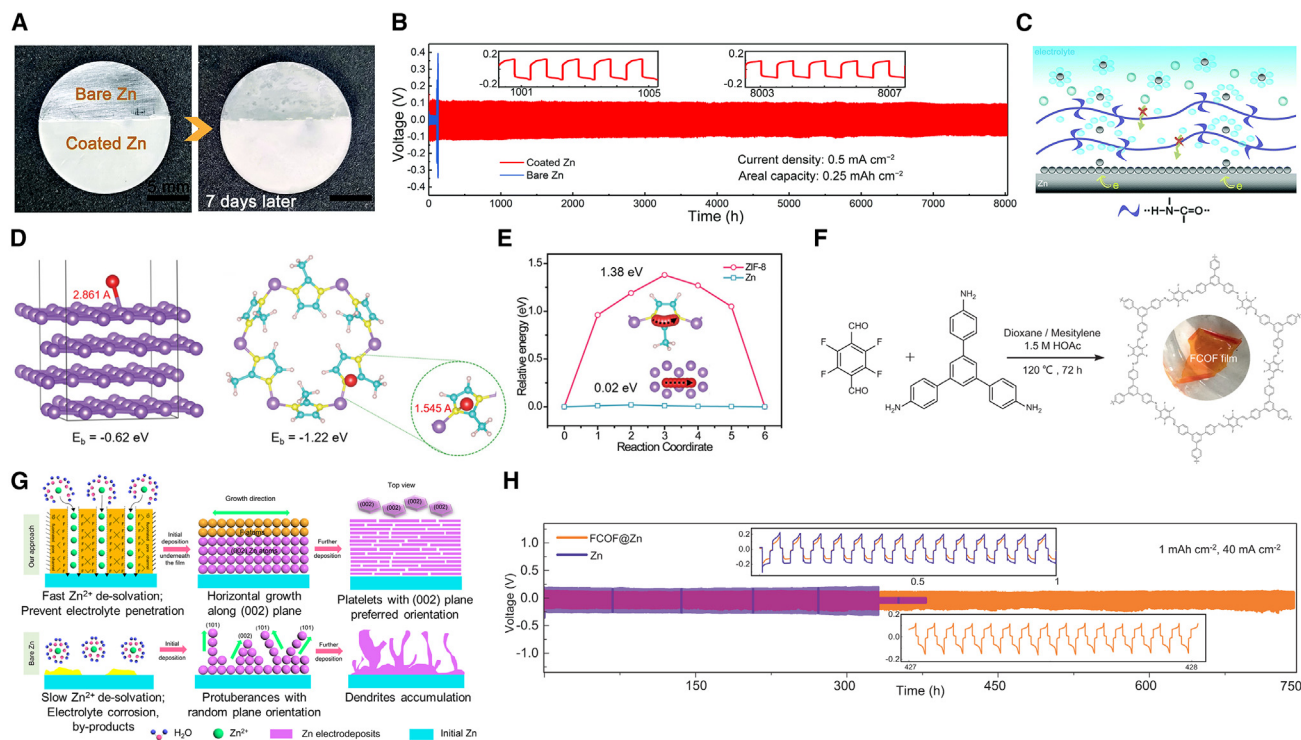


Figure 2. Organic materials coating on Zn anode

(A–C) (A) Fresh Zn plate, partially coated with a PA layer while the other half remained bare, was examined before and after immersion in water for 7 days. (B) Long-term galvanostatic cycling of symmetrical Zn cells with coated Zn. (C) Schematic diagrams for Zn deposition on the PA layer coated Zn.²² Copyright 2019 The Royal Society of Chemistry.

(D and E) (D) The calculated binding energy of Zn²⁺ on Zn (001) and ZIF-8. (E) The activation energy for Zn²⁺ to migrate from one energy minima to the other nearby minima on Zn (001) and ZIF-8.²⁶

(F–H) (F) Synthesis procedure of the FCOF film. (G) Mechanism comparison of the deposition processes for FCOF@Zn and bare Zn surfaces. (H) Cycling performance of Zn symmetric cells with or without FCOF film protection.²⁷

encapsulation of the zinc anode even during volumetric changes. This adaptability mitigates structural damage caused by zinc expansion and contraction during cycling.^{32,33}

The brightener-inspired polyamide (PA) layer has been directly applied as a solid-state interfacial coating on Zn anodes in rechargeable Zn-metal batteries (Figure 2A), enhancing lifespan (over 8,000 h) and stabilizing high areal capacity cycling (10 mAh cm⁻²), as shown in Figure 2B.²² The PA layer prevents Zn dendrite formation, blocks harmful side reactions, and significantly improves the Zn/MnO₂ battery cycle life and capacity retention (Figure 2C). MOFs and COFs materials coupling with orderly pore structure and organic coordination sites have manifested a double benefit for Zn anode stability.^{34–38} Lu et al. proposed using *in situ* grown zeolitic imidazolate framework-8 (ZIF-8) as a porous ion modulation layer to address dendrite growth and side reactions in Zn anodes.²⁶ DFT calculations further reveal that ZIF-8 enhances Zn²⁺ adsorption energy and surface diffusion barriers (Figures 2D and 2E), eliminating tip effects and ensuring uniform, dendrite-free Zn deposition. Guo et al. synthesized a fluorinated covalent organic framework (FCOF) film using 2,3,5,6-tetrafluoroterephthalaldehyde and 1,3,5-tris(4-aminophenyl)benzene as monomers through a solvothermal method,²⁷ as shown in Figure 2F.

On the one hand, when solvated zinc ions pass through the 1D channels of the COF under the influence of an electric field, the strong hydrophobicity of F repels water molecules from the solvation sheath, promoting desolvation of zinc ions. On the other hand, calculations show that the strong binding ability between F atoms and the Zn (002) plane can induce Zn growth along the (002) direction, parallel to the anode surface, thus minimizing dendrite formation, as shown in Figure 2G. Owing to these dual functions of F, the FCOF@Zn anode demonstrates stable cycling at an ultra-high current density of 40 mA/cm² for 750 h, as shown in Figure 2H.

Inorganic materials, primarily carbon materials,^{39,40} metal oxides,⁴¹ metal sulfides,^{42,43} and another metal mineral salts,^{44–46} differ from organic materials rich in functional groups. Inorganic materials mainly utilize physical confinement to regulate the diffusion and transport of Zn²⁺, influencing their nucleation and growth process.

Carbon materials, available in various forms such as graphite, carbon fiber, reduced graphene oxide (rGO), and carbon nanotubes (CNTs), offer adjustable porosity, surface area, and functionalization potential, enabling tailored designs to stabilize Zn metal anodes through their diverse physical and chemical properties.^{47–51} Chen et al. used the Langmuir-Blodgett monolayer

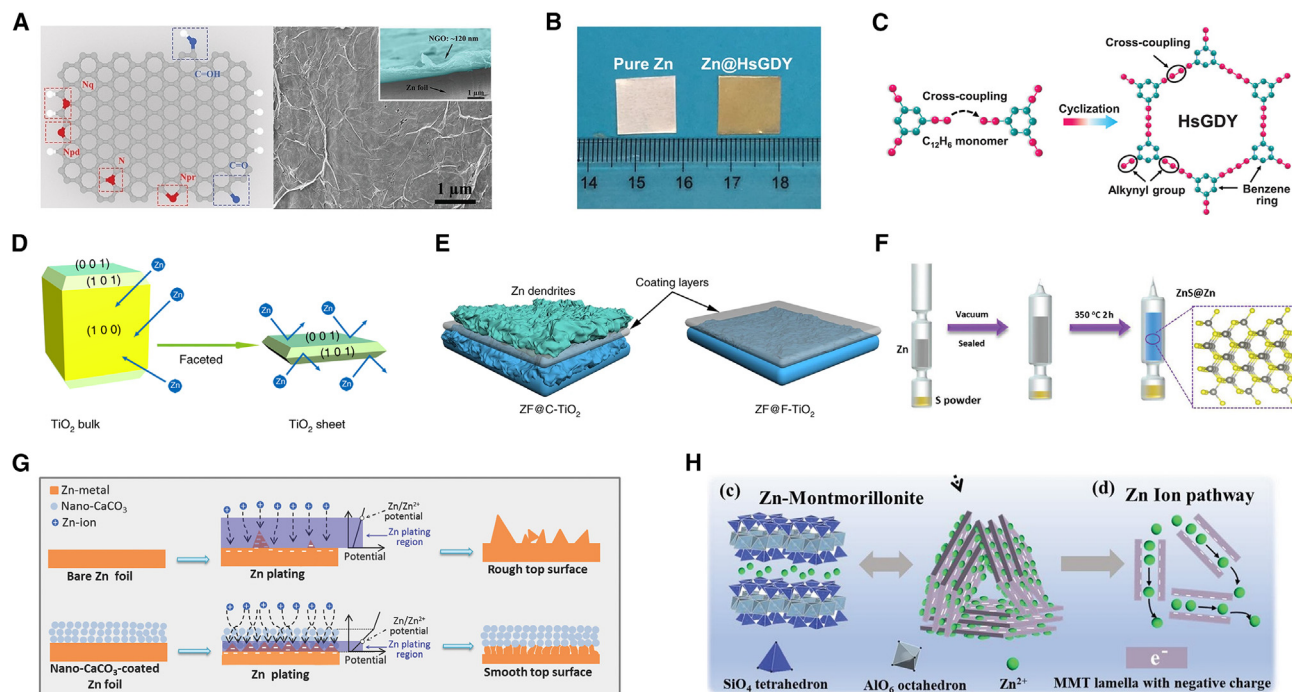


Figure 3. Inorganic materials coating on Zn anode

(A) The configuration of N- and O-doped graphene and SEM images of NGO@Zn sample.³⁹ Copyright 2021 Wiley-VCH GmbH.

(B and C) (B) Digital image showing the color evolution of Zn plate before and after HsGDY growth. (C) Schematic illustration of the synthesis of HsGDY.⁴⁰ Copyright 2020 Wiley-VCH GmbH.

(D and E) (D) Schematic illustration of the interaction between Zn and anatase TiO₂ with different exposed facets. (E) Schematic illustration of the Zn plating process with different coating layers.⁴¹

(F) Introducing the ZnS layer on the surface of the Zn metal substrate by an *in situ* strategy.⁴² Copyright 2020 Wiley-VCH GmbH.

(G) Schematic illustrations of morphology evolution for bare and nano-CaCO₃-coated Zn foils during Zn stripping/plating cycling.⁵² Copyright 2018 Wiley-VCH GmbH.

(H) Schematic of the Zn-based MMT interface inhibiting the side reactions and dendrite formation.⁴⁵ Copyright 2021 Wiley-VCH GmbH.

method to construct an ultrathin nitrogen-doped graphene oxide (NGO) film on the surface of zinc sheets,³⁹ as shown in Figure 3A. The ultrathin NGO, with a thickness of only 120 nm, improves Zn²⁺ kinetics and blocks the electrolyte, inhibiting the HER and the formation of basic zinc salt byproducts. Moreover, Zhi et al. utilized an alkyl cross-coupling reaction to generate a highly substituted graphdiyne (HSGDY) protective layer on the zinc surface, as shown in Figure 3B.⁴⁰ This layer includes large organic hexagonal rings as structural units and alternating distributions of benzene rings and diyne units. The highly ordered hexagonal ring structures have pore channels that are only 1.3–1.5 nm wide, as shown in Figure 3C. The angstrom-scale channels in the HSGDY-Zn anode guide Zn²⁺ transport along the electric field direction, creating a uniform concentration field on the electrode surface and enhancing deposition uniformity.

Metal oxides and chalcogenides, such as titanium oxide,⁴¹ aluminum oxide,⁵³ zinc oxide,⁵⁴ ZnS,⁴² SnS,⁴³ etc., offer versatility in designing protective layers with tailored properties to meet specific needs. By adjusting their structure and composition, the electronic structure and electrical conductivity can be optimized, enhancing the electrode reaction efficiency of zinc anodes. Wang et al. reveal that the crystal plane orientation of TiO₂ coatings on zinc anodes significantly impacts Zn deposition

(Figure 3D): anatase TiO₂ with the (100) plane favors Zn deposition on the coating surface, whereas TiO₂ exposing the (001) and (101) planes promotes bonding with underlying Zn, reducing dendrite formation (Figure 3E).⁴¹ This study underscores the importance of crystal orientation in developing effective protective coatings for zinc anodes. Guo et al. addressed the persistent challenges of side reactions and dendrite growth in Zn metal anodes by constructing a robust and homogeneous ZnS interphase via a vapor-solid strategy, as shown in Figure 3F.⁴² This dense ZnS film acts as a physical barrier to suppress Zn corrosion and guides uniform Zn plating/stripping beneath the protective layer, effectively preventing dendrite formation.

Inorganic salts also often acted as a functional protective layer for modified Zn anodes. Zhi Chunyi's team applied a nanoporous calcium carbonate (CaCO₃) coating to Zn anodes, using delicate pores to restrict Zn²⁺ diffusion and achieve uniform ion concentration at the interface. The insulating CaCO₃ layer directs Zn²⁺ deposition from the electrode surface rather than tip regions, promoting uniform, bottom-up deposition stabilizing cycling, as shown in Figure 3G.⁵² Li et al. developed an MMT@Zn anode by intercalating Zn²⁺ ions into the layers of montmorillonite (MMT), a layered aluminosilicate, which facilitates Zn²⁺ transport and retention through electrostatic interactions (Figure 3H). The

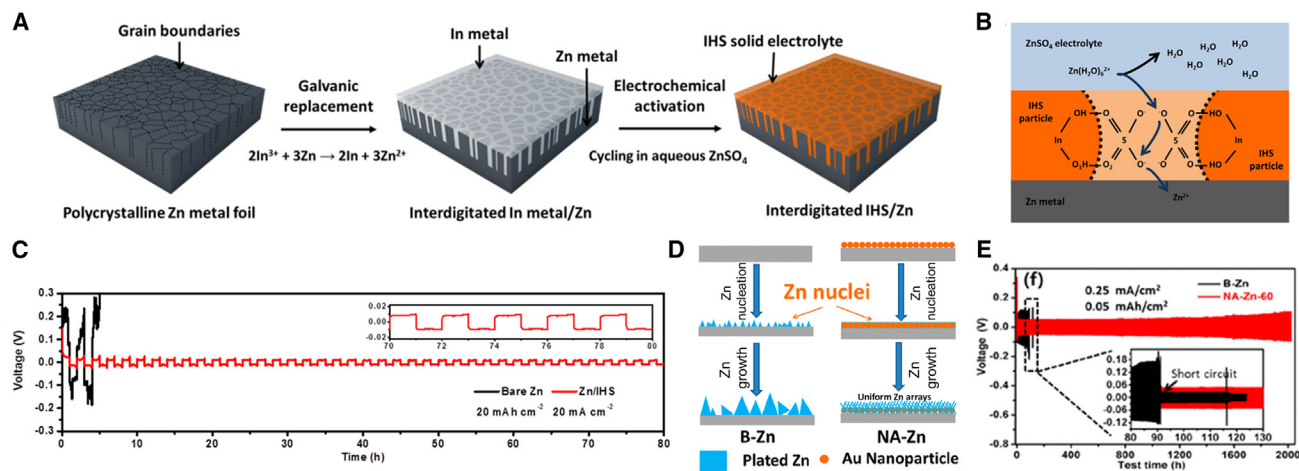


Figure 4. Metallic materials coating on Zn anode

(A–C) (A) Schematic of the fabrication of the Zn/IHS electrode. (B) Schematic illustration of the Zn^{2+} diffusion in IHS solid electrolyte on Zn metal. (C) Voltage profiles of Zn||Zn and Zn/IHS||Zn/IHS symmetrical cells.⁶⁶

(D and E) (D) Schematic illustration of the Zn stripping/plating process on a B-Zn and NA-Zn. (E) Long-term cycling profiles of Zn||Zn symmetrical cells.⁵⁷

hydrophobic MMT structure further isolates the electrolyte from the electrode surface, reducing side reactions and enhancing stability at high current densities.⁴⁵

In addition to organic and inorganic materials, metallic materials can also be used as metallic materials for zinc anodes. Various metals, including indium, copper, tin, antimony, silver, and gold, etc. have been extensively explored, yielding significant advancements in electrochemical performance.^{55–63} With their excellent electrical conductivity, the incorporation of metallic materials minimizes battery polarization, whereas metals with higher hydrogen overpotentials effectively suppress the HER.^{64,65} Sun et al. used an ion exchange reaction to coat zinc anodes with indium, which is converted during electrochemical activation to an indium hydroxide sulfate (IHS) layer, forming a Zn/IHS interface that excludes solvated Zn^{2+} ions (Figure 4A).⁶⁶ This desolvation effect within the IHS layer facilitates Zn^{2+} diffusion, reducing interfacial polarization voltage, whereas the insulating properties of IHS prevent electron transfer, thus suppressing HER and corrosion side reactions, as shown in Figure 4B. The protective layer enabled the Zn anode to maintain stable cycling for 80 h under a current density of 20 mA cm^{-2} with 20 mAh cm^{-2} capacity while exhibiting a low polarization voltage of 10 mV (Figure 4C). Zhi et al. developed an NA-Zn anode by ion sputtering nanogold (Au) particles onto a zinc substrate, where the high-curvature Au nanoparticles enhance local electric fields and act as uniform nucleation sites for Zn^{2+} , effectively preventing dendrite formation (Figure 4D).⁵⁷ This NA-Zn anode demonstrated stable cycling for over 2,000 h at 0.25 mA cm^{-2} , with the dissimilar metal layer guiding uniform Zn growth and suppressing side reactions due to its higher HER overpotential (Figure 4E).

Morphological and structural adjustments of zinc anodes

Although many of the previously discussed coating methods target flat zinc sheet electrodes, optimizing the morphology

and structure of zinc anodes is also a common approach to mitigate zinc dendrite formation. Structural modifications, such as using nanostructured materials or creating porous architectures, can enhance ion distribution and promote uniform deposition, thereby preventing dendrite formation and improving overall electrochemical performance.⁶⁷

Zhi et al. identified issues with using zinc plate anodes as working electrodes and current collectors, including imbalanced NP ratios and severe storage corrosion, as shown in Figure 5A.⁶⁸ Introducing an electroplated tin layer on the copper mitigated corrosion, allowing the Zn-P@Sn-Cu/MnO₂ cell to retain performance after 120 h of aging (Figure 5B). Li et al. developed a Zn powder/graphene (Zn-PG) anode by combining commercial zinc powder with graphene, which serves as a binder-free conductive network (Figure 5C).⁶⁹ The graphene lattice's low defect density enhances interfacial charge transfer, whereas its hexagonal structure aligns with zinc, promoting epitaxial growth and suppressing dendrite formation (Figure 5D).

Beyond replacing flat zinc anodes with zinc powder anodes, numerous studies have investigated electrodes with novel structural designs. Guan et al. employed a two-step chemical vapor deposition process to load nitrogen-doped vertical graphene (N-VG) nanosheets onto carbon cloth (CC), followed by zinc electroplating to create a Zn@N-VG@CC anode structure (Figure 5E).⁷⁰ The nitrogen atoms in N-VG attract Zn^{2+} ions, whereas the 3D vertical graphene array enhances electric field uniformity, reducing nucleation overpotential and promoting uniform Zn nucleation. Xue et al. used inkjet printing to deposit silver nanoparticles (AgNPs) onto a 3D carbon cloth array. AgNPs serve as nucleation sites that facilitate uniform Zn nucleation and growth by forming an AgZn_3 alloy phase (Figure 5F).⁷¹

An alternative strategy for controlling zinc anode morphology involves using liquid metals. Metal deposition at the interface is a liquid-solid reaction, with the electric field effect promoting deposition at high-curvature points, thereby increasing the risk of zinc dendrite formation. Some researchers have adopted an

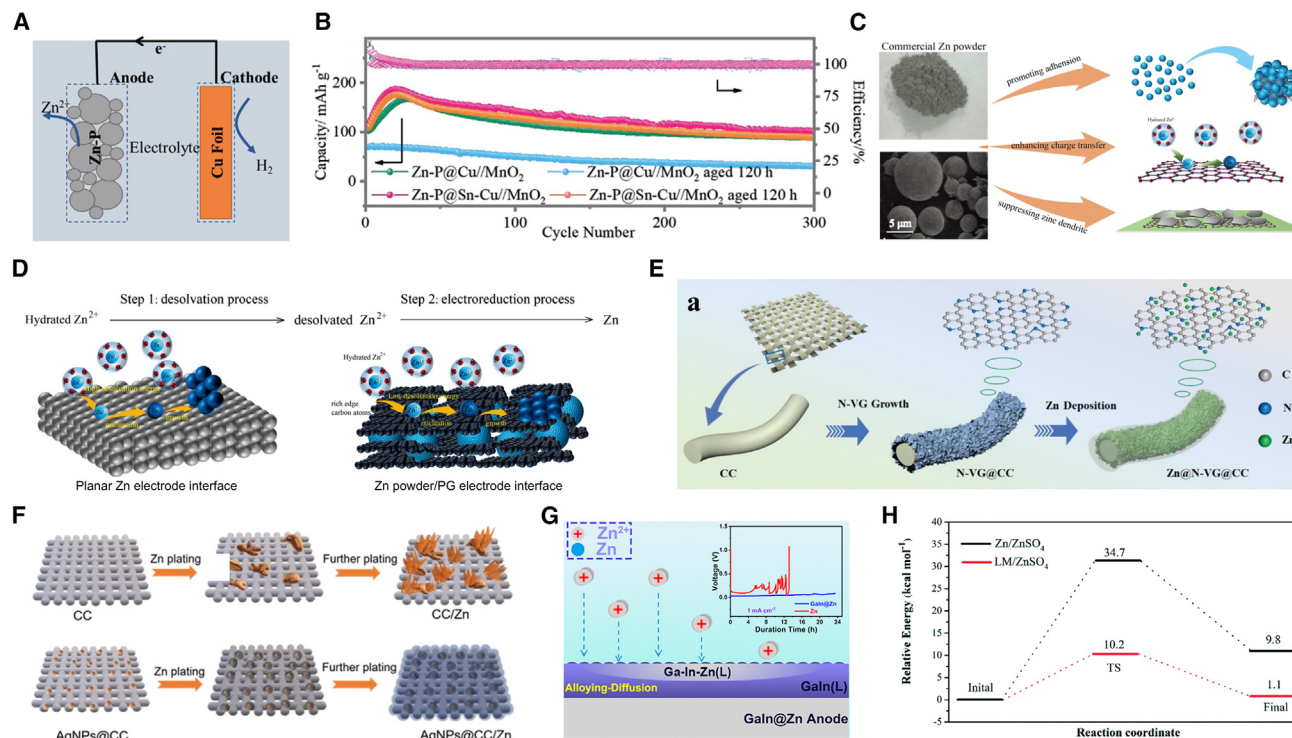


Figure 5. Examples of morphological and structural adjustments of zinc anodes

(A and B) (A) Equivalent circuit of galvanic corrosion. (B) The cycling performance of the Zn-P@Sn-Cu/MnO₂ cell for the initial state and aged for 120 h.⁶⁸ Copyright 2021 Wiley-VCH GmbH.

(C and D) (C) The design idea of using multifunctional PG to construct zinc powder anode. (D) The schematic illustration of the deposition process of zinc ion on Zn powder/PG and Zn foil electrodes.⁶⁹ Copyright 2022 Elsevier Ltd.

(E) Schematic illustrations of preparing N-VG@CC and Zn@N-VG@CC electrode.⁷⁰ Copyright 2021 Wiley-VCH GmbH.

(F) The schematic illustrations of Zn deposition on bare CC and AgNPs@CC scaffolds.⁷¹ Copyright 2021 Wiley-VCH GmbH.

(G) Dendrite-free Galn@Zn anode by alloying-diffusion synergistic strategy.⁷²

(H) Zn ion migration barrier energy from Zn and LM@Zn electrodes to the ZnSO₄ electrolyte.⁷³ Copyright 2021 The Royal Society of Chemistry.

alternative approach by using liquid alloys as the anode, leveraging the fluidity of liquid metals to create a dynamic interface. Zinc atoms can diffuse freely at both the interface and within the bulk phase, fundamentally avoiding the limitations associated with metal deposition. Ji et al. applied a layer of liquid gallium-indium (Galn) alloy to a zinc anode surface. This created a Galn@Zn anode where zinc forms a ternary alloy at the interface before diffusing inward to deposit on the zinc layer.⁷² This alloying-diffusion mechanism keeps the zinc content within the solubility limit of the liquid alloy, stabilizing the interface (Figure 5G). Zhang et al. applied a liquid Galn alloy coating on zinc to create a Galn@Zn anode, where the alloy layer lowers the Zn²⁺ diffusion barrier (Figure 5H), promoting rapid and uniform Zn nucleation.⁷³ Challenges such as the zinc content threshold in the alloy phase limited Zn²⁺ diffusion at high current densities, and the lack of comprehensive multi-element phase diagrams hinders the selection and advancement of suitable liquid alloy systems.

Another alloying strategy integrates corrosion-resistant metals with reactive zinc metal to create a stable structure that withstands mildly corrosive electrolytes. By incorporating appropriate amounts of metals or organic corrosion inhibitors into

the zinc anode, alloyed anodes can effectively inhibit the formation of unwanted by-products like Zn₄SO₄(OH)₆·nH₂O while protecting the zinc surface.^{74–77} Furthermore, this method promotes uniform zinc-ion distribution, increases charge storage capacity, reduces zinc nucleation energy, and minimizes polarization overpotentials. Using an alloying strategy, Zhou et al. demonstrated that intermetallic compounds (IMCs) preferentially distributed at grain boundaries can suppress intergranular corrosion and stabilize the zinc anode.⁷⁷ This thermodynamic stability, combined with the hybrid nucleation and growth mode induced by reduced Gibbs free energy, enables dense Zn deposition, achieving 99.85% Coulombic efficiency over 4,000 cycles and stable cycling in pouch cells for 500 cycles.

Electrolyte regulation

The electrolyte in ZMBs, composed of zinc salts, solvents, and additives, is critical for determining ion transport behavior, electrochemical stability, and Coulombic efficiency. Adjusting its composition through strategies such as concentrated electrolytes,^{78–80} water-in-salt electrolytes (WISEs),^{81–87} and deep eutectic electrolytes (DEEs)^{88–92} has effectively addressed challenges in aqueous ZMBs. Furthermore, incorporating targeted

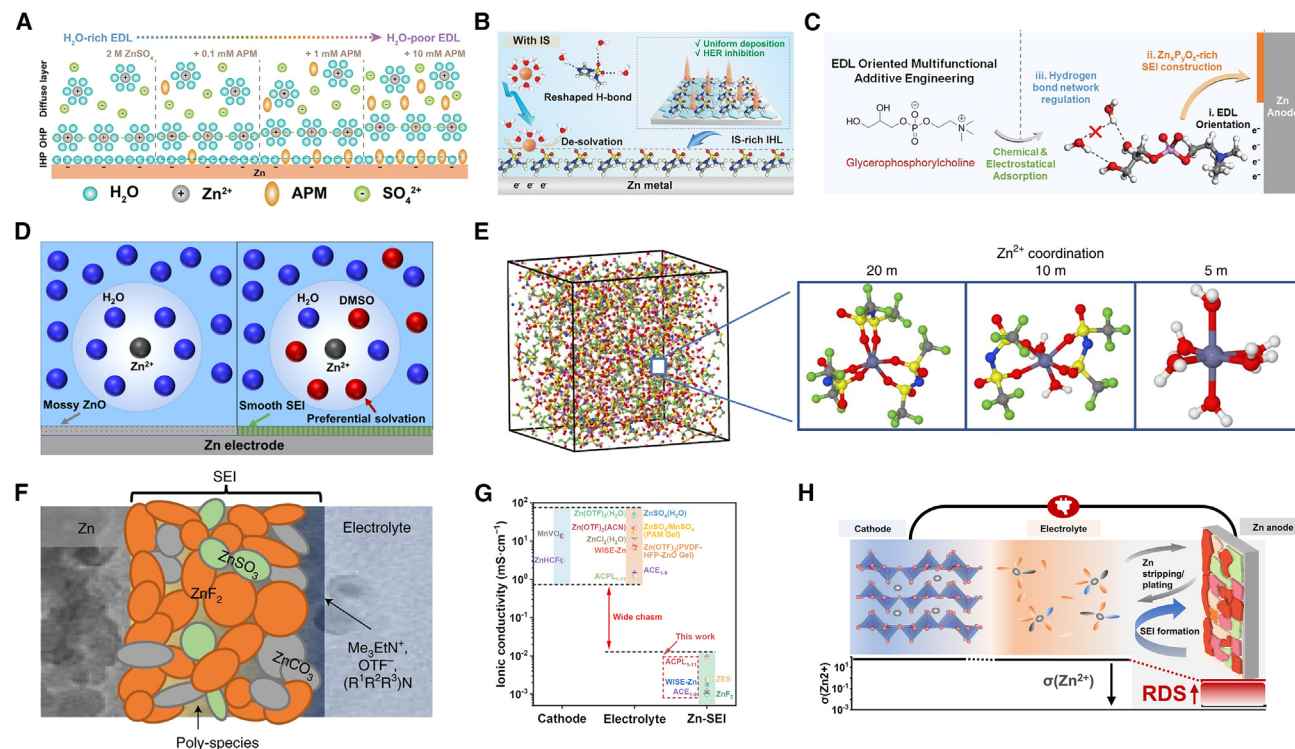


Figure 6. Electrolyte regulation

(A) Schematic illustrations of the EDL structure at the Zn anode/electrolyte interface in different electrolytes.⁹⁵ Copyright 2024 The Royal Society of Chemistry.
(B) The IHL, the desolvation process of zinc ions, and corresponding interfacial reactions of the zinc metal anode in the electrolyte with IS.⁹⁴ Copyright 2024 Wiley-VCH GmbH.
(C) A schematic representation of the EDL-oriented eutectic additive design for stabilizing Zn anodes, along with characterizations illustrating the EDL orientation of the GPC molecule.⁹⁷ Copyright 2024 Wiley-VCH GmbH.
(D) Scheme of Zn²⁺ solvation structure and zinc surface passivation in H₂O (left) and H₂O-DMSO (right) solvents.⁹⁰
(E) The MD simulation for super-concentrated electrolyte (1 m Zn(TFSI)₂ + 20 m LiTFSI).⁸⁵ Copyright 2018 Springer Science & Business Media.
(F) A schematic depiction of the proposed Zn²⁺-conducting SEI.⁹⁹ Copyright 2021 Springer Science & Business Media.
(G and H) (G) Comparison of Zn²⁺ conductivity of typical cathode materials, electrolytes, and SEIs. (H) The schematic showing Zn²⁺ conduction in SEI as the rate-determining step in ZMBs.⁹ Copyright 2024 Elsevier Ltd.

electrolyte additives into these electrolyte systems offers a low-cost and eco-friendly method to enhance zinc anode stability further and extend calendar life.⁹³ Current research on electrolyte design can be categorized into three main approaches: (1) modulating the electric double layer (EDL), (2) solvation structure optimization, (3) facilitating *in situ* SEI formation. These advancements provide valuable insights into solving interfacial challenges and improving the performance and scalability of ZMBs.

Modulating the electric double layer

The EDL plays a critical role in governing the interfacial properties of zinc-based batteries by mediating interactions between the zinc anode and the electrolyte. Structurally, the EDL comprises the inner Helmholtz plane (IHP) and the outer Helmholtz plane (OHP), where solvated zinc ions undergo desolvation and reduction, facilitating zinc plating and stripping. However, challenges such as high desolvation energy, HER, and parasitic side reactions within the EDL result in uneven zinc ion flux and dendrite formation, ultimately compromising battery performance. Modulating the EDL provides a promising strategy to enhance interfacial stability and improve the electrochemical ef-

iciency of zinc-based batteries. Incorporating small amounts of additives into aqueous electrolytes effectively tunes the EDL while preserving the intrinsic properties of the original electrolyte, ensuring compatibility with existing cathode materials system.^{94–98}

Aspartame (APM) was used to regulate the EDL structure at the Zn/electrolyte interface, transitioning from H₂O-rich to H₂O-poor conditions to study its effects on Zn plating/stripping processes.⁹⁵ Reducing H₂O in the EDL suppressed dendrite formation and side reactions by increasing Zn nucleation overpotential and limiting Zn's contact with active water. However, excessive H₂O reduction impeded Zn stripping and caused dead Zn formation (Figure 6A). An optimal H₂O-poor EDL, achieved with 1 mM APM, balanced these effects, enabling Zn||Zn symmetric cells to achieve an ultra-long lifespan and stable operation. Li et al. proposed a functional group assembly strategy to design electrolyte additives for regulating the EDL of zinc metal anodes, effectively mitigating side reactions and enabling uniform Zn deposition (Figure 6B).⁹⁴ By combining an imidazole group with strong adsorption capability and a sulfone

group that facilitates Zn^{2+} desolvation, the designed additive (N, N-dimethyl-1H-imidazole-1-sulfonamide, IS) forms a molecular protective layer in the inner Helmholtz layer, suppressing H_2O -induced side reactions and promoting compact Zn nucleation. Huang et al. developed a eutectic additive with EDL-oriented fragments to reconfigure the Zn anode/electrolyte interface in ZMBs, achieving significant stability improvements.⁹⁷ The highly polarized glycerophosphorylcholine (GPC) molecules regulate the EDL structure by modifying the hydrogen bond network to suppress HER and enrich the interface with negative charge density, forming a $\text{Zn}_x\text{P}_y\text{O}_z$ -rich SEI that prevents dendrite growth in charge-rich regions, as shown in Figure 6C.

Solvation structure optimization

In aqueous zinc ion electrolytes, organic molecules and water molecules act as Lewis bases, competing to coordinate with Zn^{2+} . To effectively replace water in the primary solvation shell and suppress the HER during zinc ion reduction, the polar functional groups of organic molecules must exhibit stronger Zn^{2+} -binding energies compared to water molecules, which can be evaluated using DFT calculations by analyzing surface electrostatic potentials that reflect electron cloud densities. The incorporation of organic molecules not only replaces water molecules in the solvation shell but also forms stronger hydrogen bonds with water due to their more negative surface electrostatic potentials, disrupting and weakening the original hydrogen-bond network among water molecules, thereby reducing water activity in the bulk electrolyte. Moreover, increasing the salt concentration in the electrolyte also allows certain anions to enter the primary solvation shell, displacing water molecules (Figure 6D).^{90,100} Therefore, manipulating the solution structure, particularly the primary solvation sheath structure of Zn^{2+} , is crucial for enhancing Coulombic efficiency and suppressing dendrite formation. The use of additives, which offers a wide range of options and ease of implementation, makes this approach more practical. In ZMBs, additives include organic small molecules,^{101–105} inorganic salts,^{106–110} and some polymers.^{111–115} These additives integrate into the Zn^{2+} solvation sheath, modifying its structure and enhancing performance. Yang et al. introduced triethylammonium ion (TMA) as an additive in ZnCl_2 electrolyte, enhancing Zn anode stability by forming $\text{ZnCl}_4(\text{TMA})_2$ complexes, which effectively exclude water from the solvation sheath and suppress the HER side reaction.¹¹⁶ Mao et al. introduced γ -butyrolactone (GBL) into the ZnSO_4 electrolyte, where the carbonyl group in GBL coordinates with Zn^{2+} , integrating into the solvation sheath and enhancing ion stability.¹¹⁷

Another straightforward approach to modifying the solvation structure of metal ions is by increasing salt concentration, which allows anions to replace solvent molecules in the solvation sheath—a strategy known as "water-in-salt" or super-concentrated electrolytes in lithium-ion batteries. This concept has also been applied to aqueous zinc-ion batteries, where super-concentrated electrolytes improve ion stability and suppress side reactions.⁸⁵ Wang et al. employed a super-concentrated electrolyte comprising 1M $\text{Zn}(\text{TFSI})_2$ and 21M LiTFSI, significantly altering the solvation structure of Zn^{2+} ions.⁸⁵ Molecular dynamics simulations revealed that as LiTFSI concentration increases, water molecules in the Zn^{2+} solvation sheath are progressively replaced by TFSI[−] ions, ultimately forming

$\text{Zn}(\text{TFSI})_3^-$ without any water at 20M LiTFSI (Figure 6E). In addition to $\text{Zn}(\text{TFSI})_2$ electrolytes, ZnCl_2 has also been used in super-concentrated electrolyte systems for ZMBs.^{86,118,119}

Facilitating in situ SEI formation

Using fluorinated anions as zinc salts makes CIP and AGG ion pairs crucial for facilitating *in situ* fluorine-rich SEI formation through anion reduction. Increasing the salt concentration in the electrolyte confines water molecules, gradually reducing the relative abundance of solvent-separated ion pairs (SSIP), where cations predominantly coordinate with solvent molecules. Relative abundance of contact ion pairs (CIP) and aggregated ions (AGG) increases in which metal ions directly coordinate with anions and multiple metal ions and multidentate anions form. Additionally, additives or co-solvents can undergo synchronous reduction during the zinc ion reduction process, contributing to constructing a high-performance SEI.¹²⁰ Wang et al. introduced trimethylamine tris(trifluoromethanesulfonyl) imide (Me_3EtNOTf) into $\text{Zn}(\text{OTf})_2$ electrolyte, resulting in an SEI layer confirmed by XPS and TEM, comprising ZnF_2 , ZnSO_3 , ZnCO_3 , and organic compounds (Figure 6F).⁹⁹ This SEI layer facilitated nearly 100% Coulombic efficiency and enabled the zinc anode to cycle stably for over 6,000 h at 0.5 mA/cm². Additional studies using $\text{Zn}(\text{NO}_3)_2$,¹²¹ N,N-dimethylformamide trifluoromethanesulfonate (DOTf),¹²² fluoroethylene carbonate (FEC),¹²³ 1,3-dioxolane (DOL),¹²⁴ and tetraethylammonium trifluoromethanesulfonate (EtNOTf)¹²⁵ also report effective *in situ* SEI formation, though further research is needed to precisely characterize SEI composition and formation conditions for optimized zinc anode performance.¹⁷

Inorganic components, such as fluorinated species (e.g., ZnF_2), play a critical role in stabilizing the SEI and enhancing the reversibility of zinc metal anodes by providing excellent electronic insulation and controlled ion diffusion. Furthermore, organic species, often formed from the reduction of electrolyte solvents or additives, contribute flexibility and chemical stability to the SEI. These components improve interfacial adhesion and ensure conformal coverage of the zinc surface, which is particularly important for accommodating volume changes during cycling. The combination of inorganic and organic components results in a composite SEI layer with complementary properties. Han et al. proposed a fluorine-rich double protective layer strategy using a multifunctional tetradecafluorononane-1,9-diol (TDFND) additive containing CF_2 -rich and OH-terminated groups, which preferentially adsorb on the Zn surface to regulate Zn^{2+} flux and induce uniform Zn(002) crystal plane deposition through a cross-linked $\text{Zn}(\text{OR})_2$ network.¹²⁶ The decomposition of TDFND, facilitated by its low LUMO energy, constructs a ZnF_2 -rich SEI that effectively suppresses side reactions, such as hydrogen evolution and by-product formation, ensuring long-term cycling stability and high Coulombic efficiency. Furthermore, Zhi et al. identified Zn^{2+} transport within the SEI as the limiting factor in in-cell carrier transfer kinetics for typical intercalation-type ZMBs (Figure 6G).⁹ The calculated migration barrier of Zn^{2+} in Zn_3N_2 is 0.52 eV, significantly lower than those of ZnF_2 (0.87 eV), ZnS (1.16 eV), ZnSO_3 (1.25 eV), and ZnO (2.21 eV). This remarkably low barrier facilitates faster ion transport and charge transfer, thereby enhancing Zn stripping/plating kinetics and overall battery performance. By optimizing SEI composition using an amide-based DEE with cyclic

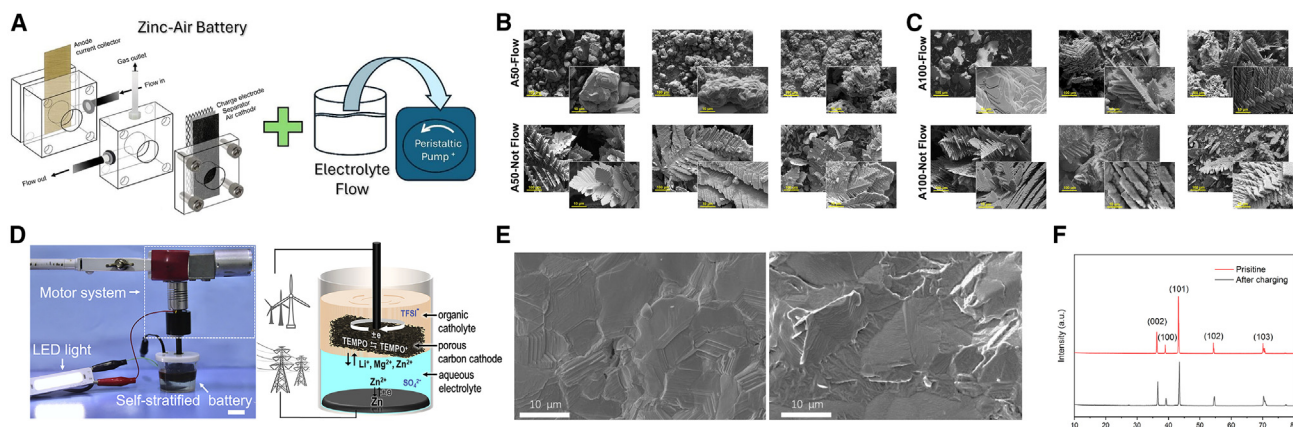


Figure 7. Flowing electrolyte

(A–C) (A) Schematic view of the ZAFBs used in the study.

(B and C) SEM images depicting the morphology of Zn deposits during charge/discharge cycling at current densities of 50 mA/cm² (B) and 100 mA/cm² (C), using flowing electrolyte (top) and static electrolyte (bottom).¹²⁷ Copyright 2024 Elsevier Ltd.

(D–F) (D) Schematic illustration of the SSB. (E) SEM Images of the Zn Anode after the 20th (left) and 150th (right) cycles (after discharge). (F) XRD of the Zn anode (pristine and after charging).¹²⁸ Copyright 2020 Elsevier Ltd.

amide additives, the formation of Zn₃N₂, a highly Zn²⁺-conductive species, was achieved, surpassing the performance of traditional ZnF₂ in promoting Zn²⁺ mobility and enhancing zinc anode stability (Figure 6H).

Flowing electrolyte

Flowing electrolytes are commonly applied in aqueous zinc flow batteries and significantly enhance the overall performance of zinc anodes by reducing concentration polarization at the anode-electrolyte interface and providing a smoother initial surface for the zinc electrode, particularly at higher current densities (Figure 7A). This promotes a more controlled and gradual evolution of the electrode structure, mitigating the detrimental effects of dendrite formation and improving the overall stability of zinc deposition. The consistent flow of electrolyte ensures more uniform zinc layer adhesion and enhances long-term cycling performance.

Kheawhom et al. investigated the impact of electrolyte flow on zinc electrodeposition and performance in zinc-air flow batteries (ZAFBs), focusing on the interplay between current density, flow rate, and their effects on electrode morphology and the ZnO passivating layer.¹²⁷ Their findings highlight that electrolyte flow at specific current densities enhances zinc morphology by reducing dendrite formation, improving deposition uniformity, and decreasing charge transfer resistance, which ultimately prolongs cycling performance. Regulating electrolyte flow can reduce internal resistance by enhancing ion transport and minimizing concentration polarization, thereby improving the overall energy efficiency of the system. Notably, the combination of electrolyte flow with a moderate current density of 50 mA/cm², and even at a higher current density of 100 mA/cm², significantly refined zinc morphology and reduced passivation (Figures 7B and 7C). In contrast to static electrolyte cells, flow electrolyte cells exhibited less dendrite growth, delayed discharge polarization, and more stable performance, highlighting the advantages of electrolyte flow for improving long-term cycling stability.

Moreover, Huang et al. developed a stirred self-stratified battery (SSB) featuring a gravity-driven, self-stratified architecture, where a zinc anode is positioned at the bottom, an aqueous electrolyte in the middle, and an organic catholyte on top.¹²⁸ The SSB uses a thick, flowing aqueous electrolyte layer to separate the zinc anode from the catholyte, effectively preventing dendrite-induced short circuits (Figure 7D). Additionally, the gravitational force and electrolyte stirring ensure that any exfoliated zinc remains on the anode surface, contributing to the battery's capacity while mitigating dendrite formation. Long-term cycling tests showed an areal capacity of 99.5 mAh/cm², corresponding to a dense 168-μm-thick zinc film, significantly surpassing the typical <40 mAh/cm² observed in conventional zinc anode batteries. SEM and XRD analyses further confirmed the stability of the zinc anode, with no signs of short-circuiting or inert by-product formation after 150 cycles, highlighting its exceptional deep charge-discharge stability (Figures 7E and 7F).

CONCLUSION AND OUTLOOK

We review the challenges zinc metal anodes face in deposition/dissolution reactions, including dendrite formation, corrosion, and side reactions in aqueous electrolytes, which critically hinder the advancement of these batteries. This study conducts an in-depth investigation into the effects of various enhancement strategies on the stability and reversibility of zinc anodes, including artificial SEI on zinc anodes, morphology and structural adjustments, electrolyte regulation, and flowing electrolyte. Thoroughly examining the mechanisms underlying performance improvements from these modification approaches offers valuable insights and guidance for advancing zinc anode design. Despite these progressions, the commercialization of RZBs demands further efforts, particularly in addressing challenges associated with large-area and high-capacity zinc deposition, where non-uniform deposition exacerbates dendrite formation and hydrogen evolution. To achieve high energy density and

exceptional cycling performance in ZMBs, further investigation into the formation and evolution of the SEI is essential. However, several critical challenges must still be addressed to establish efficient Zn metal anodes:

First, the zinc full cells should implement a lower negative-to-positive (N/P) ratio to construct zinc-ion batteries with higher energy and power densities. This requires minimizing excess zinc while integrating multiple optimization strategies, including artificial SEI layers, structural adjustments, and electrolyte regulation, to address interfacial challenges synergistically and enable scalable high-performance ZMBs.

Second, SEI layers with optimized composition and structure to facilitate higher-rate zinc deposition should be developed. A well-designed SEI can improve the uniformity of zinc deposition, reduce side reactions, and enhance the overall cycling stability of the battery.

Third, a new electrolyte system that effectively reduces HER at the zinc interface can be created. Extensive research has focused on optimizing the solvation shell structure of zinc ions, whereas relatively little attention has been directed toward the microstructural design adjustment of electrolytes. Advanced characterization tools are essential for providing deeper mechanistic insights into the microstructural evolution of electrolytes. Such insights will facilitate the development of innovative electrolytes capable of enhancing Coulombic efficiency by minimizing unwanted side reactions.

Fourth, further studies should focus on exploring and developing new zinc-ion cathode materials with higher voltage and specific capacity. Advanced cathode materials can significantly boost the overall energy density and performance of ZMBs, making them more competitive with other energy storage technologies.

Fifth, the gel and solid-state electrolytes (SSEs) represent promising advancements for zinc anodes, with the role of *in situ* SEI formation in these systems warranting detailed discussion. However, both gel and SSEs exhibit intrinsic characteristics that significantly influence SEI formation, particularly through limited anion mobility. In gel electrolytes, anions are immobilized within the polymer matrix, whereas in SSEs, their movement is restricted by the solid lattice, reducing their participation in interfacial reactions and hindering the development of substantial anion-derived SEI layers. Consequently, SEI layers in these systems are often less pronounced, and their necessity remains a subject of debate, requiring further investigation in future studies.

Finally, the commercialization of ZMBs faces economic and manufacturing challenges that require careful consideration of the cost-effectiveness of materials, such as cathode materials and electrolyte components, as well as scalable production techniques. It is essential to balance material performance with industrial feasibility, which is a critical factor for large-scale implementation. Additionally, exploring potential synergies between ZMBs and other energy storage technologies, such as lithium-ion and lead-acid batteries, could help address the demands of both residential and large-scale energy storage applications.

AUTHOR CONTRIBUTIONS

X.G. and C.Z. proposed the outline and guided the manuscript. X.G. organized the manuscript. X.G., S.Z., H.H., S.W., J.Z., and C.Z. reviewed and made sig-

nificant revisions to the article. All authors contributed to the discussion and completion of the manuscript.

DECLARATION OF INTERESTS

The authors declare no competing interests.

REFERENCES

1. Liang, Y., and Yao, Y. (2022). Designing modern aqueous batteries. *Nat. Rev. Mater.* 8, 109–122. <https://doi.org/10.1038/s41578-022-00511-3>.
2. Chao, D., Zhou, W., Xie, F., Ye, C., Li, H., Jaroniec, M., and Qiao, S.-Z. (2020). Roadmap for advanced aqueous batteries: From design of materials to applications. *Sci. Adv.* 6, eaba4098. <https://doi.org/10.1126/sciadv.aba4098>.
3. Liu, Y., Lu, X., Lai, F., Liu, T., Shearing, P.R., Parkin, I.P., He, G., and Brett, D.J. (2021). Rechargeable aqueous Zn-based energy storage devices. *Joule* 5, 2845–2903. <https://doi.org/10.1016/j.joule.2021.10.011>.
4. Jia, X., Liu, C., Neale, Z.G., Yang, J., and Cao, G. (2020). Active Materials for Aqueous Zinc Ion Batteries: Synthesis, Crystal Structure, Morphology, and Electrochemistry. *Chem. Rev.* 120, 7795–7866. <https://doi.org/10.1021/acs.chemrev.9b00628>.
5. Li, C., Jin, S., Archer, L.A., and Nazar, L.F. (2022). Toward practical aqueous zinc-ion batteries for electrochemical energy storage. *Joule* 6, 1733–1738. <https://doi.org/10.1016/j.joule.2022.06.002>.
6. Zhang, T., Tang, Y., Guo, S., Cao, X., Pan, A., Fang, G., Zhou, J., and Liang, S. (2020). Fundamentals and perspectives in developing zinc-ion battery electrolytes: a comprehensive review. *Energy Environ. Sci.* 13, 4625–4665. <https://doi.org/10.1039/d0ee02620d>.
7. Blanc, L.E., Kundu, D., and Nazar, L.F. (2020). Scientific Challenges for the Implementation of Zn-Ion Batteries. *Joule* 4, 771–799. <https://doi.org/10.1016/j.joule.2020.03.002>.
8. Xu, C., Li, B., Du, H., and Kang, F. (2012). Energetic Zinc Ion Chemistry: The Rechargeable Zinc Ion Battery. *Angew. Chem. Int. Ed.* 51, 933–935. <https://doi.org/10.1002/anie.201106307>.
9. Guo, X., Lu, J., Wang, M., Chen, A., Hong, H., Li, Q., Zhu, J., Wang, Y., Yang, S., Huang, Z., et al. (2024). Solid-electrolyte interphase governs zinc ion transfer kinetics in high-rate and stable zinc metal batteries. *Chem* 10, 3607–3621. <https://doi.org/10.1016/j.chempr.2024.07.028>.
10. Zheng, J., Yin, J., Zhang, D., Li, G., Bock, D.C., Tang, T., Zhao, Q., Liu, X., Warren, A., Deng, Y., et al. (2020). Spontaneous and field-induced crystallographic reorientation of metal electrodeposits at battery anodes. *Sci. Adv.* 6, eabb1122. <https://doi.org/10.1126/sciadv.abb1122>.
11. Zhu, M., Hu, J., Lu, Q., Dong, H., Karnaushenko, D.D., Becker, C., Karnaushenko, D., Li, Y., Tang, H., Qu, Z., et al. (2021). A Patternable and In Situ Formed Polymeric Zinc Blanket for a Reversible Zinc Anode in a Skin-Mountable Microbattery. *Adv. Mater.* 33, 2007497. <https://doi.org/10.1002/adma.202007497>.
12. Yang, Q., Li, L., Hussain, T., Wang, D., Hui, L., Guo, Y., Liang, G., Li, X., Chen, Z., Huang, Z., et al. (2022). Stabilizing Interface pH by N-Modified Graphdiyne for Dendrite-Free and High-Rate Aqueous Zn-Ion Batteries. *Angew. Chem.* 61, e202112304. <https://doi.org/10.1002/ange.202112304>.
13. Qian, X., Chen, T., Wang, Y., Zhang, Q., Li, W., and Fu, J. (2025). Revitalizing Dead Zinc with Ferrocene/Ferrocenium Redox Chemistry for Deep-Cycle Zinc Metal Batteries. *Angew. Chem. Int. Ed.* 64, e202412989. <https://doi.org/10.1002/anie.202412989>.
14. Wang, M., van Enckevort, W.J.P., Ming, N.-B., and Bennema, P. (1994). Formation of a mesh-like electrodeposited induced by electroconvection. *Nature* 367, 438–441. <https://doi.org/10.1038/367438a0>.
15. Chazalviel, J. (1990). Electrochemical aspects of the generation of ramified metallic electrodeposits. *Phys. Rev.* 42, 7355–7367. <https://doi.org/10.1103/PhysRevA.42.7355>.

16. Ding, F., Xu, W., Graff, G.L., Zhang, J., Sushko, M.L., Chen, X., Shao, Y., Engelhard, M.H., Nie, Z., Xiao, J., et al. (2013). Dendrite-Free Lithium Deposition via Self-Healing Electrostatic Shield Mechanism. *J. Am. Chem. Soc.* 135, 4450–4456. <https://doi.org/10.1021/ja312241y>.
17. Guo, X., Hong, H., Li, Q., Zhu, J., Wu, Z., Wang, Y., Yang, S., Huang, Z., Huang, Y., Li, N., and Zhi, C. (2024). Dual robust electrode-electrolyte interfaces enabled by fluorinated electrolyte for high-performance zinc metal batteries. *Matter* 7, 4014–4030. <https://doi.org/10.1016/j.matt.2024.08.002>.
18. Yang, Q., Li, Q., Liu, Z., Wang, D., Guo, Y., Li, X., Tang, Y., Li, H., Dong, B., and Zhi, C. (2020). Dendrites in Zn-Based Batteries. *Adv. Mater.* 32, 2001854. <https://doi.org/10.1002/adma.202001854>.
19. Guo, Y., Li, D., Xiong, R., and Li, H. (2019). Investigation of the temperature-dependent behaviours of Li metal anode. *Chem. Commun.* 55, 9773–9776. <https://doi.org/10.1039/C9CC04897A>.
20. Li, Q., Hong, H., Guo, X., Zhu, J., Hou, Y., Liu, C., Wang, D., Liang, G., Zhao, Y., Chen, A., et al. (2023). Distinct chemistry between Zn and Li at varied temperature. *Sci. Bull.* 68, 998–1007. <https://doi.org/10.1016/j.scib.2023.04.020>.
21. Yang, Q., Li, L., Hussain, T., Wang, D., Hui, L., Guo, Y., Liang, G., Li, X., Chen, Z., Huang, Z., et al. (2022). Stabilizing interface pH by N-modified graphdiyne for dendrite-free and high-rate aqueous Zn-ion batteries. *Angew. Chem.* 61, e202112304. <https://doi.org/10.1002/anie.202112304>.
22. Zhao, Z., Zhao, J., Hu, Z., Li, J., Li, J., Zhang, Y., Wang, C., and Cui, G. (2019). Long-life and deeply rechargeable aqueous Zn anodes enabled by a multifunctional brightener-inspired interphase. *Energy Environ. Sci.* 12, 1938–1949. <https://doi.org/10.1039/C9EE00596J>.
23. Zhang, F., Wang, C., Pan, J., Tian, F., Zeng, S., Yang, J., and Qian, Y. (2020). Polypyrrole-controlled plating/stripping for advanced zinc metal anodes. *Mater. Today Energy* 17, 100443. <https://doi.org/10.1016/j.mtener.2020.100443>.
24. Qian, X., Li, L., Wang, Y., Tian, Z., Zhong, H., Chen, W., Chen, T., and Fu, J. (2023). Versatile metallo-supramolecular polymeric interphase for highly reversible zinc metal anodes. *Energy Storage Mater.* 58, 204–214. <https://doi.org/10.1016/j.ensm.2023.03.029>.
25. Yuksel, R., Buyukcakir, O., Seong, W.K., and Ruoff, R.S. (2020). Metal-organic framework integrated anodes for aqueous zinc-ion batteries. *Adv. Energy Mater.* 10, 1904215. <https://doi.org/10.1002/aenm.201904215>.
26. Liu, X., Yang, F., Xu, W., Zeng, Y., He, J., and Lu, X. (2020). Zeolitic Imidazolate Frameworks as Zn²⁺ Modulation Layers to Enable Dendrite-Free Zn Anodes. *Adv. Sci.* 7, 2002173. <https://doi.org/10.1002/advsc.202002173>.
27. Zhao, Z., Wang, R., Peng, C., Chen, W., Wu, T., Hu, B., Weng, W., Yao, Y., Zeng, J., Chen, Z., et al. (2021). Horizontally arranged zinc platelet electrodeposits modulated by fluorinated covalent organic framework film for high-rate and durable aqueous zinc ion batteries. *Nat. Commun.* 12, 6606. <https://doi.org/10.1038/s41467-021-26947-9>.
28. Aupama, V., Kao-ian, W., Sangsawang, J., Mohan, G., Wannapaiboon, S., Mohamad, A.A., Pattanauwat, P., Sriprachubwong, C., Liu, W.-R., and Kheawhom, S. (2023). Stabilizing a zinc anode via a tunable covalent organic framework-based solid electrolyte interphase. *Nanoscale* 15, 9003–9013. <https://doi.org/10.1039/D3NR00898C>.
29. Li, L., Yang, H., Peng, H., Lei, Z., and Xu, Y. (2023). Covalent Organic Frameworks in Aqueous Zinc-Ion Batteries. *Chem. Eur. J.* 29, e202302502. <https://doi.org/10.1002/chem.202302502>.
30. Aupama, V., Sangsawang, J., Kao-ian, W., Wannapaiboon, S., Pimoei, J., yoopensuk, W., Opchoei, M., Tehrani, Z., Margadonna, S., and Kheawhom, S. (2024). Adaptive COF-PVDF composite artificial solid electrolyte interphase for stable aqueous zinc batteries. *Electrochim. Acta* 506, 145059. <https://doi.org/10.1016/j.electacta.2024.145059>.
31. Chen, Z., Wang, T., Hou, Y., Wang, Y., Huang, Z., Cui, H., Fan, J., Pei, Z., and Zhi, C. (2022). Polymeric Single-Ion Conductors with Enhanced Side-Chain Motion for High-Performance Solid Zinc-Ion Batteries. *Adv. Mater.* 34, 2207682. <https://doi.org/10.1002/adma.202207682>.
32. Cai, X., Tian, W., Zhang, Z., Sun, Y., Yang, L., Mu, H., Lian, C., and Qiu, H. (2024). Polymer Coating with Balanced Coordination Strength and Ion Conductivity for Dendrite-Free Zinc Anode. *Adv. Mater.* 36, 2307727. <https://doi.org/10.1002/adma.202307727>.
33. Hu, Z., Wang, X., Du, W., Zhang, Z., Tang, Y., Ye, M., Zhang, Y., Liu, X., Wen, Z., and Li, C.C. (2023). Crowding Effect-Induced Zinc-Enriched/Water-Lean Polymer Interfacial Layer Toward Practical Zn-Iodine Batteries. *ACS Nano* 17, 23207–23219. <https://doi.org/10.1021/acsnano.3c10081>.
34. Yang, H., Chang, Z., Qiao, Y., Deng, H., Mu, X., He, P., and Zhou, H. (2020). Constructing a Super-Saturated Electrolyte Front Surface for Stable Rechargeable Aqueous Zinc Batteries. *Angew. Chem.* 132, 9463–9467. <https://doi.org/10.1002/ange.202001844>.
35. Zhang, R., Feng, Y., Ni, Y., Zhong, B., Peng, M., Sun, T., Chen, S., Wang, H., Tao, Z., and Zhang, K. (2023). Bifunctional Interphase with Target-Distributed Desolvation Sites and Directionally Depositional Ion Flux for Sustainable Zinc Anode. *Angew. Chem.* 62, e202304503. <https://doi.org/10.1002/ange.202304503>.
36. Hu, Y.Y., Han, R.X., Mei, L., Liu, J.L., Sun, J.C., Yang, K., and Zhao, J.W. (2021). Design principles of MOF-related materials for highly stable metal anodes in secondary metal-based batteries. *Mater. Today Energy* 19, 100608. <https://doi.org/10.1016/j.mtener.2020.100608>.
37. Guo, C., Huang, X., Huang, J., Tian, X., Chen, Y., Feng, W., Zhou, J., Li, Q., Chen, Y., Li, S.-L., and Lan, Y.-Q. (2024). Zigzag Hopping Site Embedded Covalent Organic Frameworks Coating for Zn Anode. *Angew. Chem.* 63, e202403918. <https://doi.org/10.1002/ange.202403918>.
38. Liang, L., Su, L., Zhang, X., Wang, Y., Ren, W., Gao, X., Zheng, L., and Lu, F. (2024). Synergistically regulating Zn-ion flux and accelerating ion transport kinetics via zincophilic covalent organic framework interlayer for stable Zn metal anode. *Chem. Eng. J.* 485, 149813. <https://doi.org/10.1016/j.cej.2024.149813>.
39. Zhou, J., Xie, M., Wu, F., Mei, Y., Hao, Y., Huang, R., Wei, G., Liu, A., Li, L., and Chen, R. (2021). Ultrathin Surface Coating of Nitrogen-Doped Graphene Enables Stable Zinc Anodes for Aqueous Zinc-Ion Batteries. *Adv. Mater.* 33, 2101649. <https://doi.org/10.1002/adma.202101649>.
40. Yang, Q., Guo, Y., Yan, B., Wang, C., Liu, Z., Huang, Z., Wang, Y., Li, Y., Li, H., Song, L., et al. (2020). Hydrogen-Substituted Graphdiyne Ion Tunnels Directing Concentration Redistribution for Commercial-Grade Dendrite-Free Zinc Anodes. *Adv. Mater.* 32, 2001755. <https://doi.org/10.1002/adma.202001755>.
41. Zhang, Q., Luan, J., Huang, X., Wang, Q., Sun, D., Tang, Y., Ji, X., and Wang, H. (2020). Revealing the role of crystal orientation of protective layers for stable zinc anode. *Nat. Commun.* 11, 3961. <https://doi.org/10.1038/s41467-020-17752-x>.
42. Hao, J., Li, B., Li, X., Zeng, X., Zhang, S., Yang, F., Liu, S., Li, D., Wu, C., and Guo, Z. (2020). An In-Depth Study of Zn Metal Surface Chemistry for Advanced Aqueous Zn-Ion Batteries. *Adv. Mater.* 32, 2003021. <https://doi.org/10.1002/adma.202003021>.
43. Hu, Y., Fu, C., Chai, S., He, Q., Wang, Y., Feng, M., Zhang, Y., and Pan, A. (2023). Construction of zinc metal-Tin sulfide polarized interface for stable Zn metal batteries. *Adv. Powder Mater.* 2, 100093. <https://doi.org/10.1016/j.apmate.2022.100093>.
44. Kang, L., Cui, M., Jiang, F., Gao, Y., Luo, H., Liu, J., Liang, W., and Zhi, C. (2018). Nanoporous CaCO₃ coatings enabled uniform Zn stripping/plating for long-life zinc rechargeable aqueous batteries. *Adv. Energy Mater.* 8, 1801090. <https://doi.org/10.1002/aenm.201801090>.
45. Yan, H., Li, S., Nan, Y., Yang, S., and Li, B. (2021). Ultrafast Zinc-Ion-Conductor Interface toward High-Rate and Stable Zinc Metal Batteries. *Adv. Energy Mater.* 11, 2100186. <https://doi.org/10.1002/aenm.202100186>.

46. Yang, Y., Liu, C., Lv, Z., Yang, H., Cheng, X., Zhang, S., Ye, M., Zhang, Y., Chen, L., Zhao, J., and Li, C.C. (2021). Redistributing Zn-ion flux by inter-layer ion channels in Mg-Al layered double hydroxide-based artificial solid electrolyte interface for ultra-stable and dendrite-free Zn metal anodes. *Energy Storage Mater.* 41, 230–239. <https://doi.org/10.1016/j.ensm.2021.06.002>.
47. Lu, Q., Jie, Y., Meng, X., Omar, A., Mikhailova, D., Cao, R., Jiao, S., Lu, Y., and Xu, Y. (2021). Carbon materials for stable Li metal anodes: challenges, solutions, and outlook. *Carbon Energy* 3, 957–975. <https://doi.org/10.1002/cey2.147>.
48. Zhou, J., Xie, M., Wu, F., Mei, Y., Hao, Y., Li, L., and Chen, R. (2022). Encapsulation of metallic Zn in a hybrid MXene/graphene aerogel as a stable Zn anode for foldable Zn-ion batteries. *Adv. Mater.* 34, 2106897. <https://doi.org/10.1002/adma.202106897>.
49. Abouali, M., Adhami, S., Haris, S.A., and Yuksel, R. (2024). On the Dendrite-Suppressing Effect of Laser-Processed Polylactic Acid-Derived Carbon Coated Zinc Anode in Aqueous Zinc Ion Batteries. *Angew. Chem. Int. Ed.* 63, e202405048. <https://doi.org/10.1002/anie.202405048>.
50. Xie, Z.H., Yuan, Y.F., Yao, Z.J., Zhu, M., Guo, S.Y., and Du, P.F. (2024). Regulating horizontal lamellar Zn to uniformly deposit under and on the hollow porous carbon nanosphere coating for dendrite-free metal Zn anode. *Chem. Eng. J.* 484, 149601. <https://doi.org/10.1016/j.cej.2024.149601>.
51. Guo, X., Peng, Q., Shin, K., Zheng, Y., Tunmee, S., Zou, C., Zhou, X., and Tang, Y. (2024). Construction of a Composite Sn-DLC Artificial Protective Layer with Hierarchical Interfacial Coupling Based on Gradient Coating Technology Toward Robust Anodes for Zn Metal Batteries. *Adv. Energy Mater.* 14, 2402015. <https://doi.org/10.1002/aenm.202402015>.
52. Kang, L., Cui, M., Jiang, F., Gao, Y., Luo, H., Liu, J., Liang, W., and Zhi, C. (2018). Nanoporous CaCO₃ Coatings Enabled Uniform Zn Stripping/Plating for Long-Life Zinc Rechargeable Aqueous Batteries. *Adv. Energy Mater.* 8, 1801090. <https://doi.org/10.1002/aenm.201801090>.
53. Zheng, J., Huang, Z., Zeng, Y., Liu, W., Wei, B., Qi, Z., Wang, Z., Xia, C., and Liang, H. (2022). Electrostatic Shielding Regulation of Magnetron Sputtered Al-Based Alloy Protective Coatings Enables Highly Reversible Zinc Anodes. *Nano Lett.* 22, 1017–1023. <https://doi.org/10.1021/acs.nanolett.1c03917>.
54. Ma, C., Yang, K., Zhao, S., Xie, Y., Liu, C., Chen, N., Wang, C., Wang, D., Zhang, D., Shen, Z.X., and Du, F. (2023). Recyclable and Ultrafast Fabrication of Zinc Oxide Interface Layer Enabling Highly Reversible Dendrite-Free Zn Anode. *ACS Energy Lett.* 8, 1201–1208. <https://doi.org/10.1021/acsenergylett.2c02735>.
55. Han, D., Wu, S., Zhang, S., Deng, Y., Cui, C., Zhang, L., Long, Y., Li, H., Tao, Y., Weng, Z., et al. (2020). A corrosion-resistant and dendrite-free zinc metal anode in aqueous systems. *Small* 16, 2001736. <https://doi.org/10.1002/sml.202001736>.
56. Li, S., Fu, J., Miao, G., Wang, S., Zhao, W., Wu, Z., Zhang, Y., and Yang, X. (2021). Toward planar and dendrite-free Zn electrodepositions by regulating Sn-crystal textured surface. *Adv. Mater.* 33, 2008424. <https://doi.org/10.1002/adma.202008424>.
57. Cui, M., Xiao, Y., Kang, L., Du, W., Gao, Y., Sun, X., Zhou, Y., Li, X., Li, H., Jiang, F., and Zhi, C. (2019). Quasi-Isolated Au Particles as Heterogeneous Seeds To Guide Uniform Zn Deposition for Aqueous Zinc-Ion Batteries. *ACS Appl. Energy Mater.* 2, 6490–6496. <https://doi.org/10.1021/acsaem.9b01063>.
58. Lu, Q., Liu, C., Du, Y., Wang, X., Ding, L., Omar, A., and Mikhailova, D. (2021). Uniform Zn deposition achieved by Ag coating for improved aqueous zinc-ion batteries. *ACS Appl. Mater. Interfaces* 13, 16869–16875. <https://doi.org/10.1021/acsaami.0c22911>.
59. Yu, H., Chen, Y., Wang, H., Ni, X., Wei, W., Ji, X., and Chen, L. (2022). Engineering multi-functionalized molecular skeleton layer for dendrite-free and durable zinc batteries. *Nano Energy* 99, 107426. <https://doi.org/10.1016/j.nanoen.2022.107426>.
60. Gong, Z., Jiang, K., Wang, P., Liu, X., Wang, D., Ye, K., Zhu, K., Yan, J., Wang, G., and Cao, D. (2022). Stable and dendrite-free Zn anode with artificial desolvation interface layer toward high-performance Zn-ion capacitor. *J. Energy Chem.* 72, 143–148. <https://doi.org/10.1016/j.jechem.2022.05.017>.
61. Cai, Z., Ou, Y., Wang, J., Xiao, R., Fu, L., Yuan, Z., Zhan, R., and Sun, Y. (2020). Chemically resistant Cu–Zn/Zn composite anode for long cycling aqueous batteries. *Energy Storage Mater.* 27, 205–211. <https://doi.org/10.1016/j.ensm.2020.01.032>.
62. Miao, Z., Du, M., Li, H., Zhang, F., Jiang, H., Sang, Y., Li, Q., Liu, H., and Wang, S. (2021). Constructing nano-channeled tin layer on metal zinc for high-performance zinc-ion batteries anode. *EcoMat* 3, e12125. <https://doi.org/10.1002/eom2.12125>.
63. Zhang, Y., Wang, G., Yu, F., Xu, G., Li, Z., Zhu, M., Yue, Z., Wu, M., Liu, H.-K., Dou, S.-X., and Wu, C. (2021). Highly reversible and dendrite-free Zn electrodeposition enabled by a thin metallic interfacial layer in aqueous batteries. *Chem. Eng. J.* 416, 128062. <https://doi.org/10.1016/j.cej.2020.128062>.
64. Guo, W., Zhang, Y., Tong, X., Wang, X., Zhang, L., Xia, X., and Tu, J. (2021). Multifunctional tin layer enabled long-life and stable anode for aqueous zinc-ion batteries. *Mater. Today Energy* 20, 100675. <https://doi.org/10.1016/j.mtener.2021.100675>.
65. Wang, G., Yao, Q., Dong, J., Ge, W., Wang, N., Bai, Z., Yang, J., and Dou, S. (2024). In situ Construction of Multifunctional Surface Coatings on Zinc Metal for Advanced Aqueous Zinc–Iodine Batteries. *Adv. Energy Mater.* 14, 2303221. <https://doi.org/10.1002/aenm.202303221>.
66. Cai, Z., Ou, Y., Zhang, B., Wang, J., Fu, L., Wan, M., Li, G., Wang, W., Wang, L., Jiang, J., et al. (2021). A Replacement Reaction Enabled Interdigitated Metal/Solid Electrolyte Architecture for Battery Cycling at 20 mA cm^{−2} and 20 mAh cm^{−2}. *J. Am. Chem. Soc.* 143, 3143–3152. <https://doi.org/10.1021/jacs.0c11753>.
67. Jin, S., Shao, Y., Gao, X., Chen, P., Zheng, J., Hong, S., Yin, J., Joo, Y.L., and Archer, L.A. (2022). Designing interphases for practical aqueous zinc flow batteries with high power density and high areal capacity. *Sci. Adv.* 8, eabq4456. <https://doi.org/10.1126/sciadv.abq4456>.
68. Li, Q., Wang, Y., Mo, F., Wang, D., Liang, G., Zhao, Y., Yang, Q., Huang, Z., and Zhi, C. (2021). Calendar Life of Zn Batteries Based on Zn Anode with Zn Powder/Current Collector Structure. *Adv. Energy Mater.* 11, 2003931. <https://doi.org/10.1002/aenm.202003931>.
69. Du, W., Huang, S., Zhang, Y., Ye, M., and Li, C.C. (2022). Enable commercial Zinc powders for dendrite-free Zinc anode with improved utilization rate by pristine graphene hybridization. *Energy Storage Mater.* 45, 465–473. <https://doi.org/10.1016/j.ensm.2021.12.007>.
70. Cao, Q., Gao, H., Gao, Y., Yang, J., Li, C., Pu, J., Du, J., Yang, J., Cai, D., Pan, Z., et al. (2021). Regulating Dendrite-Free Zinc Deposition by 3D Zincophilic Nitrogen-Doped Vertical Graphene for High-Performance Flexible Zn-Ion Batteries. *Adv. Funct. Mater.* 31, 2103922. <https://doi.org/10.1002/adfm.202103922>.
71. Chen, T., Wang, Y., Yang, Y., Huang, F., Zhu, M., Ang, B.T.W., and Xue, J.M. (2021). Heterometallic Seed-Mediated Zinc Deposition on Inkjet Printed Silver Nanoparticles Toward Foldable and Heat-Resistant Zinc Batteries. *Adv. Funct. Mater.* 31, 2101607. <https://doi.org/10.1002/adfm.202101607>.
72. Liu, C., Luo, Z., Deng, W., Wei, W., Chen, L., Pan, A., Ma, J., Wang, C., Zhu, L., Xie, L., et al. (2021). Liquid Alloy Interlayer for Aqueous Zinc-Ion Battery. *ACS Energy Lett.* 6, 675–683. [https://doi.org/10.1021/acseenergylett.0c02569](https://doi.org/10.1021/acsenergylett.0c02569).
73. Jia, H., Wang, Z., Dirican, M., Qiu, S., Chan, C.Y., Fu, S., Fei, B., and Zhang, X. (2021). A liquid metal assisted dendrite-free anode for high-performance Zn-ion batteries. *J. Mater. Chem. A* 9, 5597–5605. <https://doi.org/10.1039/D0TA11828A>.
74. Huang, Y., Chang, Z., Liu, W., Huang, W., Dong, L., Kang, F., and Xu, C. (2022). Layer-by-layer zinc metal anodes to achieve long-life zinc-ion

- batteries. *Chem. Eng. J.* 431, 133902. <https://doi.org/10.1016/j.cej.2021.133902>.
75. Liu, B., Wang, S., Wang, Z., Lei, H., Chen, Z., and Mai, W. (2020). Novel 3D Nanoporous Zn–Cu Alloy as Long-Life Anode toward High-Voltage Double Electrolyte Aqueous Zinc-Ion Batteries. *Small* 16, 2001323. <https://doi.org/10.1002/sml.202001323>.
76. Wang, S.-B., Ran, Q., Yao, R.-Q., Shi, H., Wen, Z., Zhao, M., Lang, X.-Y., and Jiang, Q. (2020). Lamella-nanostructured eutectic zinc–aluminum alloys as reversible and dendrite-free anodes for aqueous rechargeable batteries. *Nat. Commun.* 11, 1634. <https://doi.org/10.1038/s41467-020-15478-4>.
77. Zhao, Y., Guo, S., Chen, M., Lu, B., Zhang, X., Liang, S., and Zhou, J. (2023). Tailoring grain boundary stability of zinc–titanium alloy for long-lasting aqueous zinc batteries. *Nat. Commun.* 14, 7080. <https://doi.org/10.1038/s41467-023-42919-7>.
78. Zhou, J., Shan, L., Wu, Z., Guo, X., Fang, G., and Liang, S. (2018). Investigation of V2O5 as a low-cost rechargeable aqueous zinc ion battery cathode. *Chem. Commun.* 54, 4457–4460. <https://doi.org/10.1039/c8cc02250j>.
79. Li, C., Yuan, W., Li, C., Wang, H., Wang, L., Liu, Y., and Zhang, N. (2021). Boosting Li3V2(PO4)3 cathode stability using a concentrated aqueous electrolyte for high-voltage zinc batteries. *Chem. Commun.* 57, 4319–4322. <https://doi.org/10.1039/D0CC08115A>.
80. Olbasa, B.W., Fenta, F.W., Chiu, S.-F., Tsai, M.-C., Huang, C.-J., Jote, B.A., Beyene, T.T., Liao, Y.-F., Wang, C.-H., Su, W.-N., et al. (2020). High-Rate and Long-Cycle Stability with a Dendrite-Free Zinc Anode in an Aqueous Zn-Ion Battery Using Concentrated Electrolytes. *ACS Appl. Energy Mater.* 3, 4499–4508. <https://doi.org/10.1021/acsaem.0c00183>.
81. Wang, L., Yan, S., Quilty, C.D., Kuang, J., Dunkin, M.R., Ehrlich, S.N., Ma, L., Takeuchi, K.J., Takeuchi, E.S., and Marschillok, A.C. (2021). Achieving Stable Molybdenum Oxide Cathodes for Aqueous Zinc-Ion Batteries in Water-in-Salt Electrolyte. *Adv. Mater. Interfac.* 8, 2002080. <https://doi.org/10.1002/admi.202002080>.
82. Tang, X., Wang, P., Bai, M., Wang, Z., Wang, H., Zhang, M., and Ma, Y. (2021). Unveiling the Reversibility and Stability Origin of the Aqueous V2O5–Zn Batteries with a ZnCl2 “Water-in-Salt” Electrolyte. *Adv. Sci.* 8, 2102053. <https://doi.org/10.1002/adv.202102053>.
83. Zhang, Y., Wan, G., Lewis, N.H.C., Mars, J., Bone, S.E., Steinrück, H.-G., Lukatskaya, M.R., Weadock, N.J., Bajdich, M., Borodin, O., et al. (2021). Water or Anion? Uncovering the Zn2+ Solvation Environment in Mixed Zn(TFSI)2 and LiTFSI Water-in-Salt Electrolytes. *ACS Energy Lett.* 6, 3458–3463. <https://doi.org/10.1021/acsenenergylett.1c01624>.
84. Hong, J.J., Zhu, L., Chen, C., Tang, L., Jiang, H., Jin, B., Gallagher, T.C., Guo, Q., Fang, C., and Ji, X. (2019). A Dual Plating Battery with the Iodine/[ZnIx(OH2)4-x]2-(x) Cathode. *Angew. Chem. Int. Ed. Engl.* 58, 15910–15915. <https://doi.org/10.1002/anie.201909324>.
85. Wang, F., Borodin, O., Gao, T., Fan, X., Sun, W., Han, F., Faraone, A., Dura, J.A., Xu, K., and Wang, C. (2018). Highly reversible zinc metal anode for aqueous batteries. *Nat. Mater.* 17, 543–549. <https://doi.org/10.1038/s41563-018-0063-z>.
86. Zhang, Q., Ma, Y., Lu, Y., Li, L., Wan, F., Zhang, K., and Chen, J. (2020). Modulating electrolyte structure for ultralow temperature aqueous zinc batteries. *Nat. Commun.* 11, 4463. <https://doi.org/10.1038/s41467-020-18284-0>.
87. Wang, R., Yao, M., Yang, M., Zhu, J., Chen, J., and Niu, Z. (2023). Synergistic modulation on ionic association and solvation structure by electron-withdrawing effect for aqueous zinc-ion batteries. *Proc. Natl. Acad. Sci. USA* 120, e2221980120. <https://doi.org/10.1073/pnas.2221980120>.
88. Yang, W., Du, X., Zhao, J., Chen, Z., Li, J., Xie, J., Zhang, Y., Cui, Z., Kong, Q., Zhao, Z., et al. (2020). Hydrated Eutectic Electrolytes with Ligand-Oriented Solvation Shells for Long-Cycling Zinc-Organic Batteries. *Joule* 4, 1557–1574. <https://doi.org/10.1016/j.joule.2020.05.018>.
89. Qiu, H., Du, X., Zhao, J., Wang, Y., Ju, J., Chen, Z., Hu, Z., Yan, D., Zhou, X., and Cui, G. (2019). Zinc anode-compatible in-situ solid electrolyte interphase via cation solvation modulation. *Nat. Commun.* 10, 5374. <https://doi.org/10.1038/s41467-019-13436-3>.
90. Cao, L., Li, D., Hu, E., Xu, J., Deng, T., Ma, L., Wang, Y., Yang, X.-Q., and Wang, C. (2020). Solvation Structure Design for Aqueous Zn Metal Batteries. *J. Am. Chem. Soc.* 142, 21404–21409. <https://doi.org/10.1021/jacs.0c09794>.
91. Ming, F., Zhu, Y., Huang, G., Emwas, A.-H., Liang, H., Cui, Y., and Alshar-eef, H.N. (2022). Co-Solvent Electrolyte Engineering for Stable Anode-Free Zinc Metal Batteries. *J. Am. Chem. Soc.* 144, 7160–7170. <https://doi.org/10.1021/jacs.1c12764>.
92. Han, D., Cui, C., Zhang, K., Wang, Z., Gao, J., Guo, Y., Zhang, Z., Wu, S., Yin, L., Weng, Z., et al. (2021). A non-flammable hydrous organic electrolyte for sustainable zinc batteries. *Nat. Sustain.* 5, 205–213. <https://doi.org/10.1038/s41893-021-00800-9>.
93. Yang, Z., Sun, Y., Li, J., He, G., and Chai, G. (2024). Noncovalent Interactions-Driven Self-Assembly of Polyanionic Additive for Long Anti-Calendar Aging and High-Rate Zinc Metal Batteries. *Adv. Sci.* 11, 2404513. <https://doi.org/10.1002/adv.202404513>.
94. Liu, L., Wang, X., Hu, Z., Wang, X., Zheng, Q., Han, C., Xu, J., Xu, X., Liu, H.-K., Dou, S.-X., and Li, W. (2024). Electric Double Layer Regulator Design through a Functional Group Assembly Strategy towards Long-Lasting Zinc Metal Batteries. *Angew. Chem. Int. Ed.* 63, e202405209. <https://doi.org/10.1002/anie.202405209>.
95. Qi, K., Liang, P., Wei, S., Ao, H., Ding, X., Chen, S., Fan, Z., Wang, C., Song, L., Wu, X., et al. (2024). Trade-off between H2O-rich and H2O-poor electric double layers enables highly reversible Zn anodes in aqueous Zn-ion batteries. *Energy Environ. Sci.* 17, 2566–2575. <https://doi.org/10.1039/D4EE00147H>.
96. Lin, C., He, L., Xiong, P., Lin, H., Lai, W., Yang, X., Xiao, F., Sun, X.-L., Qian, Q., Liu, S., et al. (2023). Adaptive Ionization-Induced Tunable Electric Double Layer for Practical Zn Metal Batteries over Wide pH and Temperature Ranges. *ACS Nano* 17, 23181–23193. <https://doi.org/10.1021/acsnano.3c09774>.
97. Lyu, H., Zhao, S., Liao, C., Li, G., Zhi, J., and Huang, F. (2024). Electric Double Layer Oriented Eutectic Additive Design toward Stable Zn Anodes with a High Depth of Discharge. *Adv. Mater.* 36, 2400976. <https://doi.org/10.1002/adma.202400976>.
98. Hu, B., Chen, T., Wang, Y., Qian, X., Zhang, Q., and Fu, J. (2024). Reconfiguring the Electrolyte Network Structure with Bio-Inspired Cryoprotective Additive for Low-Temperature Aqueous Zinc Batteries. *Adv. Energy Mater.* 14, 2401470. <https://doi.org/10.1002/aenm.202401470>.
99. Cao, L., Li, D., Pollard, T., Deng, T., Zhang, B., Yang, C., Chen, L., Vatanmanu, J., Hu, E., Hourwitz, M.J., et al. (2021). Fluorinated interphase enables reversible aqueous zinc battery chemistries. *Nat. Nanotechnol.* 16, 902–910. <https://doi.org/10.1038/s41565-021-00905-4>.
100. Yang, H., Chang, Z., Qiao, Y., Deng, H., Mu, X., He, P., and Zhou, H. (2020). Constructing a Super-Saturated Electrolyte Front Surface for Stable Rechargeable Aqueous Zinc Batteries. *Angew. Chem. Int. Ed.* 59, 9377–9381. <https://doi.org/10.1002/anie.202001844>.
101. Sun, K.E.K., Hoang, T.K.A., Doan, T.N.L., Yu, Y., Zhu, X., Tian, Y., and Chen, P. (2017). Suppression of dendrite formation and corrosion on zinc anode of secondary aqueous batteries. *ACS Appl. Mater. Interfaces* 9, 9681–9687. <https://doi.org/10.1021/acsaami.6b16560>.
102. Zeng, X., Xie, K., Liu, S., Zhang, S., Hao, J., Liu, J., Pang, W.K., Liu, J., Rao, P., Wang, Q., et al. (2021). Bio-inspired design of an *in situ* multi-functional polymeric solid–electrolyte interphase for Zn metal anode cycling at 30 mA cm⁻² and 30 mA h cm⁻². *Energy Environ. Sci.* 14, 5947–5957. <https://doi.org/10.1039/d1ee01851e>.
103. Yang, F., Yuwono, J.A., Hao, J., Long, J., Yuan, L., Wang, Y., Liu, S., Fan, Y., Zhao, S., Davey, K., and Guo, Z. (2022). Understanding H₂ evolution electrochemistry to minimize solvated water impact on Zinc-anode

- performance. *Adv. Mater.* 34, 2206754. <https://doi.org/10.1002/adma.202206754>.
104. Shang, Y., Kumar, P., Musso, T., Mittal, U., Du, Q., Liang, X., and Kundu, D. (2022). Long-life Zn anode enabled by low volume concentration of a benign electrolyte additive. *Adv. Funct. Mater.* 32, 2200606. <https://doi.org/10.1002/adfm.202200606>.
105. Qin, H., Kuang, W., Hu, N., Zhong, X., Huang, D., Shen, F., Wei, Z., Huang, Y., Xu, J., and He, H. (2022). Building metal-molecule interface towards stable and reversible Zn metal anodes for aqueous rechargeable zinc batteries. *Adv. Funct. Mater.* 32, 2206695. <https://doi.org/10.1002/adfm.202206695>.
106. Kim, M., Shin, S.J., Lee, J., Park, Y., Kim, Y., Kim, H., and Choi, J.W. (2022). Cationic Additive with a Rigid Solvation Shell for High-Performance Zinc Ion Batteries. *Angew. Chem.* 61, e202211589. <https://doi.org/10.1002/anie.202211589>.
107. Huang, C., Zhao, X., Hao, Y., Yang, Y., Qian, Y., Chang, G., Zhang, Y., Tang, Q., Hu, A., and Chen, X. (2022). Self-Healing SeO₂ Additives Enable Zinc Metal Reversibility in Aqueous ZnSO₄ Electrolytes. *Adv. Funct. Mater.* 32, 2112091. <https://doi.org/10.1002/adfm.202112091>.
108. Liu, D.S., Zhang, Z., Zhang, Y., Ye, M., Huang, S., You, S., Du, Z., He, J., Wen, Z., Tang, Y., et al. (2023). Manipulating OH[−]-Mediated Anode-Cathode Cross-Communication Toward Long-Life Aqueous Zinc-Vanadium Batteries. *Angew. Chem. Int. Ed.* 62, e202215385. <https://doi.org/10.1002/anie.202215385>.
109. Lin, C., Yang, X., Xiong, P., Lin, H., He, L., Yao, Q., Wei, M., Qian, Q., Chen, Q., and Zeng, L. (2022). High-rate, large capacity, and long life dendrite-free Zn metal anode enabled by trifunctional electrolyte additive with a wide temperature range. *Adv. Sci.* 9, 2201433. <https://doi.org/10.1002/advs.202201433>.
110. Li, Y., Wu, P., Zhong, W., Xie, C., Xie, Y., Zhang, Q., Sun, D., Tang, Y., and Wang, H. (2021). A progressive nucleation mechanism enables stable zinc stripping-plating behavior. *Energy Environ. Sci.* 14, 5563–5571. <https://doi.org/10.1039/D1EE01861B>.
111. Wu, Y., Zhu, Z., Shen, D., Chen, L., Song, T., Kang, T., Tong, Z., Tang, Y., Wang, H., and Lee, C.S. (2022). Electrolyte engineering enables stable Zn-ion deposition for long-cycling life aqueous Zn-ion batteries. *Energy Storage Mater.* 45, 1084–1091. <https://doi.org/10.1016/j.ensm.2021.11.003>.
112. Wang, H., Li, H., Tang, Y., Xu, Z., Wang, K., Li, Q., He, B., Liu, Y., Ge, M., Chen, S., et al. (2022). Stabilizing Zn anode interface by simultaneously manipulating the thermodynamics of Zn nucleation and overpotential of hydrogen evolution. *Adv. Funct. Mater.* 32, 2207898. <https://doi.org/10.1002/adfm.202207898>.
113. Wang, B., Zheng, R., Yang, W., Han, X., Hou, C., Zhang, Q., Li, Y., Li, K., and Wang, H. (2022). Synergistic Solvation and Interface Regulations of Eco-Friendly Silk Peptide Additive Enabling Stable Aqueous Zinc-Ion Batteries. *Adv. Funct. Mater.* 32, 2112693. <https://doi.org/10.1002/adfm.202112693>.
114. Liu, J., Song, W., Wang, Y., Wang, S., Zhang, T., Cao, Y., Zhang, S., Xu, C., Shi, Y., Niu, J., and Wang, F. (2022). A polyamino acid with zincophilic chains enabling high-performance Zn anodes. *J. Mater. Chem. A* 10, 20779–20786. <https://doi.org/10.1039/D2TA05528G>.
115. Cao, Z., Zhu, X., Gao, S., Xu, D., Wang, Z., Ye, Z., Wang, L., Chen, B., Li, L., Ye, M., and Shen, J. (2022). Ultraprecise Zinc Anode by Simultaneously Manipulating Solvation Sheath and Inducing Oriented Deposition with PEG Stability Promoter. *Small* 18, 2103345. <https://doi.org/10.1002/smll.202103345>.
116. Yao, R., Qian, L., Sui, Y., Zhao, G., Guo, R., Hu, S., Liu, P., Zhu, H., Wang, F., Zhi, C., and Yang, C. (2022). A Versatile Cation Additive Enabled Highly Reversible Zinc Metal Anode. *Adv. Energy Mater.* 12, 2102780. <https://doi.org/10.1002/aenm.202102780>.
117. Huang, H., Xie, D., Zhao, J., Rao, P., Choi, W.M., Davey, K., and Mao, J. (2022). Boosting Reversibility and Stability of Zn Anodes via Manipulation of Electrolyte Structure and Interface with Addition of Trace Organic Molecules. *Adv. Energy Mater.* 12, 2202419. <https://doi.org/10.1002/aenm.202202419>.
118. Zhang, C., Holoubek, J., Wu, X., Daniyar, A., Zhu, L., Chen, C., Leonard, D.P., Rodríguez-Pérez, I.A., Jiang, J.-X., Fang, C., and Ji, X. (2018). A ZnCl₂ water-in-salt electrolyte for a reversible Zn metal anode. *Chem. Commun.* 54, 14097–14099. <https://doi.org/10.1039/C8CC07730D>.
119. Tang, X., Wang, P., Bai, M., Wang, Z., Wang, H., Zhang, M., and Ma, Y. (2021). Unveiling the reversibility and stability origin of the aqueous V2O₅-Zn batteries with a ZnCl₂ “water-in-salt” electrolyte. *Adv. Sci.* 8, 2102053. <https://doi.org/10.1002/advs.202102053>.
120. Hu, B., Wang, Y., Qian, X., Chen, W., Liang, G., Chen, J., Zhao, J., Li, W., Chen, T., and Fu, J. (2023). Colloid Electrolyte with Weakly Solvated Structure and Optimized Electrode/Electrolyte Interface for Zinc Metal Batteries. *ACS Nano* 17, 12734–12746. <https://doi.org/10.1021/acsnano.3c03638>.
121. Li, D., Cao, L., Deng, T., Liu, S., and Wang, C. (2021). Design of a Solid Electrolyte Interphase for Aqueous Zn Batteries. *Angew. Chem. Int. Ed.* 60, 13035–13041. <https://doi.org/10.1002/anie.202103390>.
122. Li, C., Shyamsunder, A., Hoane, A.G., Long, D.M., Kwok, C.Y., Kotula, P.G., Zavadil, K.R., Gewirth, A.A., and Nazar, L.F. (2022). Highly reversible Zn anode with a practical areal capacity enabled by a sustainable electrolyte and superacid interfacial chemistry. *Joule* 6, 1103–1120. <https://doi.org/10.1016/j.joule.2022.04.017>.
123. Xie, D., Sang, Y., Wang, D.-H., Diao, W.-Y., Tao, F.-Y., Liu, C., Wang, J.-W., Sun, H.-Z., Zhang, J.-P., and Wu, X.-L. (2023). ZnF₂-Riched Inorganic/Organic Hybrid SEI: *in situ*-Chemical Construction and Performance-Improving Mechanism for Aqueous Zinc-Ion Batteries. *Angew. Chem. Int. Ed.* 62, e202216934. <https://doi.org/10.1002/anie.202216934>.
124. Du, H., Wang, K., Sun, T., Shi, J., Zhou, X., Cai, W., and Tao, Z. (2022). Improving zinc anode reversibility by hydrogen bond in hybrid aqueous electrolyte. *Chem. Eng. J.* 427, 131705. <https://doi.org/10.1016/j.cej.2021.131705>.
125. Zhao, X., Dong, N., Yan, M., and Pan, H. (2023). Unraveling the Interfacial Chemistry for Highly Reversible Aqueous Zn Ion Batteries. *ACS Appl. Mater. Interfaces* 15, 4053–4060. <https://doi.org/10.1021/acsaami.2c19022>.
126. Li, T., Hu, S., Wang, C., Wang, D., Xu, M., Chang, C., Xu, X., and Han, C. (2023). Engineering Fluorine-rich Double Protective Layer on Zn Anode for Highly Reversible Aqueous Zinc-ion Batteries. *Angew. Chem. Int. Ed.* 62, e202314883. <https://doi.org/10.1002/anie.202314883>.
127. Khezri, R., Motlagh, S.R., Etesami, M., Pakawani, P., Olaru, S., Somwangthanaroj, A., and Kheawhom, S. (2024). Balancing current density and electrolyte flow for improved zinc-air battery cyclability. *Appl. Energy* 376, 124239. <https://doi.org/10.1016/j.apenergy.2024.124239>.
128. Meng, J., Tang, Q., Zhou, L., Zhao, C., Chen, M., Shen, Y., Zhou, J., Feng, G., Shen, Y., and Huang, Y. (2020). A Stirred Self-Stratified Battery for Large-Scale Energy Storage. *Joule* 4, 953–966. <https://doi.org/10.1016/j.joule.2020.03.011>.